Progress in Biomaterials (2022) 11:163–191
https://doi.org/10.1007/s40204-022-00189-4

REVIEW PAPER

Progress in manufacturing and processing of degradable Fe-based implants: a review

V. P. Muhammad Rabeeh[1] · T. Hanas[1,2]

Received: 15 February 2022 / Accepted: 1 May 2022 / Published online: 18 May 2022

Abstract

Biodegradable metals have gained vast attention as befitting candidates for developing degradable metallic implants. Such implants are primarily employed for temporary applications and are expected to degrade or resorbed after the tissue is healed. Fe-based materials have generated considerable interest as one of the possible biodegradable metals. Like other biometals such as Mg and Zn, Fe exhibits good biocompatibility and biodegradability. The versatility in the mechanical behaviour of Fe-based materials makes them a better choice for load-bearing applications. However, the very low degradation rate of Fe in the physiological environment needs to be improved to make it compatible with tissue growth. Several studies on tailoring the degradation behaviour of Fe in the human body are already reported. Majority of these works include studies on the effect of manufacturing and processing techniques on biocompatibility and biodegradability. This article focuses on a comprehensive review and analysis of the various manufacturing and processing techniques so far reported for developing biodegradable iron-based orthopaedic implants. The current status of research in the field is neatly presented, and a summary of the works is included in the article for the benefit of researchers in the field to contextualise their research and effectively find the lacunae in the existing scholarship.

Keywords Iron · Biodegradable metals · Surface modification · In vitro · Orthopaedic implant · Biomaterials · Biometals

Introduction

Since the eighteenth century, metals have been used for biomedical surgical implant applications due to their outstanding mechanical properties and durability (Niinomi 2008). Titanium (Ti), stainless steel (SS) and cobalt-chromium (Co–Cr)-based "bio-inert" alloys are commonly used as metallic biomaterials. The mechanical properties such as tensile strength, fracture toughness, ductility and wear resistance make these metals suitable for implant applications. Permanent metallic stents and joint replacement implants are mainly developed using these alloys (Niinomi 2008; Lévesque et al. 2008; Moravej and Mantovani 2011; Zheng et al. 2014; Ito et al. 2015; Kumar et al. 2019; Leo Kumar and Avinash 2020). Although these conventional alloys are considered to be biocompatible, unfavourable conditions may cause a toxic element release in the region. This can cause sensitivity towards different metal components or allergic reactions such as localised eczema near the implant site (Chaturvedi 2013). In temporary implant applications, these are to be removed by a second surgery once the tissue is healed (Zhang et al. 2010; Chen and Thouas 2015). A second surgery increases the associated cost and raises the chances for hospital-acquired infections (Kirchhoff et al. 2008). Post-operative problems such as nerve injury, infection, incomplete removal, and impaired wound healing have been reported occasionally following implant removal surgery (Reith et al. 2015). Moreover, factors such as age and the patient's health condition can hinder the possibility of such a second surgery. The slow rate of bone healing in older people leads to screw holes in the cortical bone area after implant removal. Such holes are a concern as they can be subjected to stress concentration resulting in bone fracture (Brooks et al. 1970). The concept of biodegradable metals (BMs) is seen as one of the promising alternatives to the second surgery. BMs are expected to degrade at a

✉ T. Hanas
hanas@nitc.ac.in

[1] Nanomaterials Research Laboratory, School of Materials Science and Engineering, National Institute of Technology Calicut, Kozhikode 673601, India

[2] Department of Mechanical Engineering, National Institute of Technology Calicut, Kozhikode 673601, India

predetermined rate in the physiological environment without any harmful effect on tissue and thereby help to avoid the second surgery.

The implants made of BMs are expected to degrade and disappear from the disease site with little residue (Wong et al. 2012; Hermawan 2018; Li et al. 2019a). The ideal biodegradable material shall have a desirable degradation rate compatible with the regeneration rate of the tissues. Shuai et al. 2019a reported that the degradation rate of BMs used in bone repair needs to be between 0.2 and 0.5 mmpy (Sheikh et al. 2015). However, the degradation rate will have to conform to the new bone growth rate to ensure the progressive transfer of load to the healing bone, minimising the disadvantages of stress shielding. When the implant degrades, its strength decreases and the load is progressively transferred to the recovering bone tissue (Waizy et al. 2013). The biodegradation of metals inside the body depends primarily on interaction with its environment. The reaction of some metals can also bring benefits for biomedical applications (Zheng et al. 2014). The BMs can contain vital metallic elements that the human body tissues could gradually absorb and also help in achieving the desired level of degradation in vivo (Seal et al. 2009; Zheng et al. 2014). Thus, one can see that the concept of biodegradable metallic implants challenges the conventional paradigm that metallic biomaterials should be resistant to degradation (Bauer et al. 2013).

Degradable metallic biomaterials currently proposed mainly include magnesium- (Mg), zinc- (Zn) and iron- (Fe) based systems (Loffredo et al. 2018; Shuai et al. 2019a; Garimella et al. 2019; Rahim et al. 2020; Yang et al. 2020; Md Yusop et al. 2021). While the Mg-based materials rapidly degrade (at a rate ranging from 0.8 to 2.7 mmpy) in the physiological environment (Zberg et al. 2009; Dorozhkin 2014; Shuai et al. 2019a), Fe-based systems exhibit a very slow degradation rate (less 0.2 mmpy) as shown in Fig. 1 (Hermawan et al. 2010a; Sing et al. 2015). Unlike Mg-based BMs, Zn-based BMs degrade in the physiological environment without the release of hydrogen gas. They also exhibit degradation rates between 0.1 and 0.3 mmpy, which is compatible with desired degradation rate for BMs as reported in the literature (Kabir et al. 2021). However, due to the insufficient mechanical characteristics of Zn, its usage is limited for the majority of medical applications such as stents and orthopaedic implants (Vojtěch et al. 2011). In addition, the comparatively poor fatigue strength and low-temperature recrystallisation, proneness to creep and increased vulnerability to the natural ageing of Zn and Zn alloys potentially lead to poor performance of medical implants during the storage and functioning period (Li et al. 2019b).

Fe-based systems have the required mechanical characteristics, good formability, and acceptable biocompatibility. However, they often degrade relatively slowly with degradation rates much below clinical criteria and hence

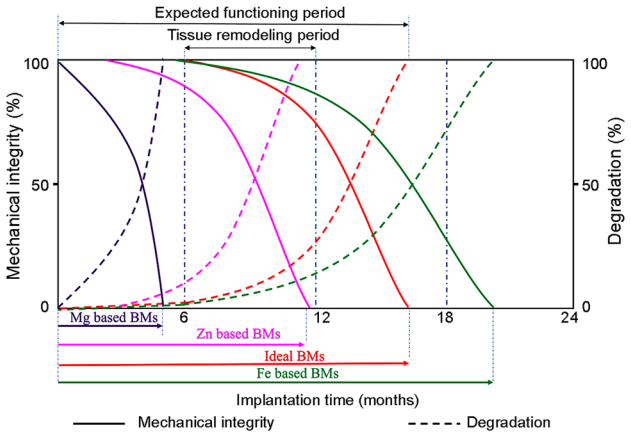

Fig. 1 The schematic representation of degradation of BMs and variations in mechanical integrity during the tissue healing process (Hermawan et al. 2010a; Mostaed et al. 2016)

potentially create identical issues as raised with conventional implant materials. Table 1 summarises the major advantages and disadvantages of Mg-, Zn- and Fe-based biodegradable metals.

The ongoing research on Fe-based systems mainly focuses on increasing the degradation rate in the physiological environment.

Fe is an essential element of the human body as it has many vital roles and functions in the human body (Papanikolaou and Pantopoulos, 2005). For adults, the average oral consumption of iron is 12–18 mg/day and approximately 10% of the same is extracted by the digestive tract. Based on stomach distress as a side effect, the highest permissible intake level of iron, is limited to 45 mg/day (Seiler and Sigel 1988; Trumbo et al. 2001). The majority part of iron available is used to produce haemoglobin, and the liver stores additional intakes in the form of ferritin and haemosiderin (Saito 2014). The dynamic distribution of iron in the human body is shown in Fig. 2.

In the physiological environment, degradation of Fe takes place by electrochemical reactions as shown in the following equations (Zheng et al. 2014, 2017):

$$\mathrm{Fe} \rightarrow \mathrm{Fe}^{2+} + 2\mathrm{e}^{-}(\text{anodic reaction}), \tag{1}$$

$$\mathrm{O_2} + 2\mathrm{H_2O} + 4\mathrm{e}^{-} \rightarrow 4\mathrm{OH}^{-}(\text{cathodic reaction}). \tag{2}$$

In the solution, this Fe^{2+} and OH^{-} will combine to form ferrous hydroxide:

$$\mathrm{Fe}^{2+} + 2\mathrm{OH}^{-}\mathrm{Fe(OH)_2} \downarrow . \tag{3}$$

Due to the alkalisation of the solution and the presence of oxygen in the physiological fluid, some ferrous hydroxide transforms to ferric hydroxide as per the following reactions:

Table 1 Major advantages and disadvantages of Mg-, Zn- and Fe-based biodegradable metals

Biodegradable metal	Advantages	Disadvantages
Mg-based BMs	Biodegradable Biocompatible Promote biomineralisation and osseointegration Density and elastic modulus close to that of human bone and thereby reduce the chances of stress shielding MRI compatible An essential element for the human body	Extremely high degradation rate H_2 gas evolution by degradation Local rise of pH near the implant site Poor mechanical strength for load-bearing application Premature loss of mechanical integrity
Zn-based BMs	Biodegradable Acceptable biocompatibility Good processability No H_2 gas evolution by degradation Non-toxic degradation products	Poor mechanical strength Proneness to creep Age hardening
Fe-based BMs	Biodegradable High tensile strength and formability Acceptable biocompatibility MRI compatible (in austenitic phase) No H_2 gas evolution by degradation	Very low degradation rate High elastic modulus leads to stress shielding Non-MRI compatible for ferromagnetic Fe and its alloys

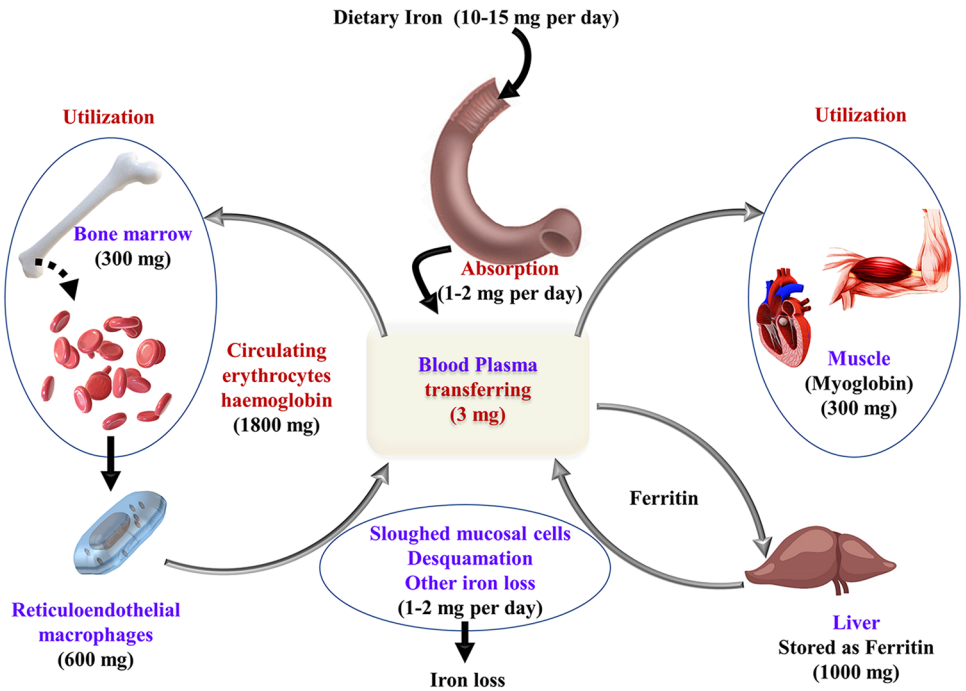

Fig. 2 Dynamic distribution of iron in the body

$$4Fe(OH)_2 + O_2 + 2H_2O4Fe(OH)_3 \downarrow, \quad (4)$$

$$Fe(OH)_2 + 2FeO(OH) + Fe_3O_4 \downarrow + H_2O. \quad (5)$$

Figure 3 depicts a schematic diagram of the degradation mechanism of Fe-based biodegradable materials in the physiological environment. As illustrated in Fig. 3a, the reactions (1)–(5) indicated above occur spontaneously at the sites where a galvanic couple exists. Metallic iron undergoes oxidation instantly upon contact with bodily fluid due to the anodic reaction (1). The liberated electrons are used in the cathodic reaction equivalent to the reduction of dissolved oxygen as shown in reaction (2). As shown in Fig. 3, this reaction occurs along with the adsorption of organic

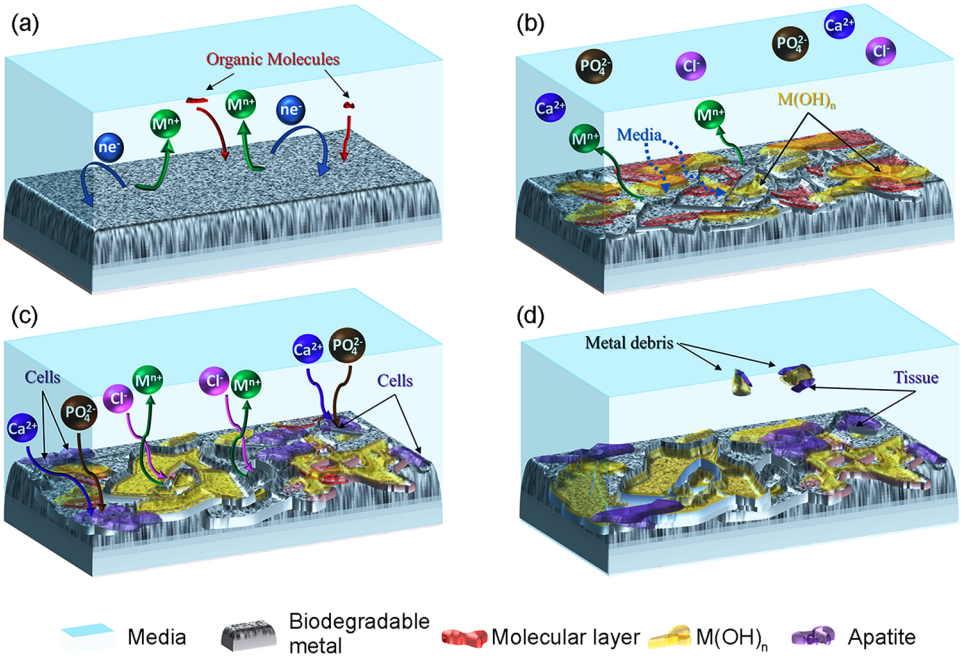

Fig. 3 Degradation mechanism of Fe-based BMs

molecules such as lipids, proteins and amino acids as well as the formation of degradation products as per the reactions (3)–(5). Due to the high concentrations of inorganic ions such as Cl^- in the body fluid, the hydroxide layer breakdown persistently, which leads to continuous degradation (Paramitha et al. 2016). Aside from the corrosion product layer, cells cling to the surface and then proliferate to form the tissues. The irregular fragments may occasionally fall from the degraded surface and get removed from the site as shown in Fig. 3d.

The formation of calcium phosphate (apatite) layer and that of hydroxide and oxide on the surface of Fe contribute to a reduction in the degradation rate during the early period of dynamic immersion (Zhu et al. 2009b). However, a degradation layer on the iron surface would not be a worry in the in vivo implantation as reported by Wegener et al. (2021). It is reported that the degradation products were removed by macrophages and no harmful effects were observed as a result of the local accumulation. It is also reported that the degradation products of Fe display no apparent toxicity to human tissue, and excessive Fe ions will be transported through body fluid and promptly excreted through sloughed mucosal cells, sweat and desquamation of skin cells and hair (Peuster et al. 2001; Ulum et al. 2014; Scarcello and Lison 2020).

The combination of biodegradability and superior mechanical properties makes Fe a perfect choice for load-bearing applications. The key benefits and limitations of Fe-based systems are given in Table 2.

As mentioned earlier, researchers have reported plethora of manufacturing and processing techniques to accelerate the rate of degradation, improve biological response and tune the mechanical behaviour of Fe for degradable implant applications. This paper reviews all the significant works reported to this date with a special emphasis

Table 2 Benefits and limitations of Fe-based systems as degradable implant

Benefits of Fe-based system	Limitations of Fe-based system
Biocompatible and biodegradable in the physiological environment	Slow degradation rate in the physiological environment
Good strength and toughness	High stiffness compared to that of natural bone and can lead to the stress shielding phenomena
Fe is an essential cation required for human metabolism and acts as a co-factor for many enzymes and haemoglobin synthesis	Chances of formation of insoluble degradation products (IDP) built up near implantation site may harm the nearby tissue
Hyper-iron cases are rare	
Good machinability index and dimensional stability are crucial for developing complex geometries for orthopaedic applications	

on the manufacturing route and processing techniques adopted.

Manufacturing of iron-based biodegradable metals

The manufacturing methods attempted to develop biodegradable metallic materials from Fe-based systems can be broadly grouped as powder metallurgy, casting, electrodeposition, additive manufacturing and others as shown in Fig. 4. The advantages and disadvantages of each method for manufacturing Fe-based biodegradable devices are summarised in Table 3.

Powder metallurgy

Powder metallurgy (PM) is one of the most common methods for developing Fe-based BMs (Hermawan et al. 2007; 2008, 2010b; Cheng and Zheng, 2013; Zheng et al. 2014;

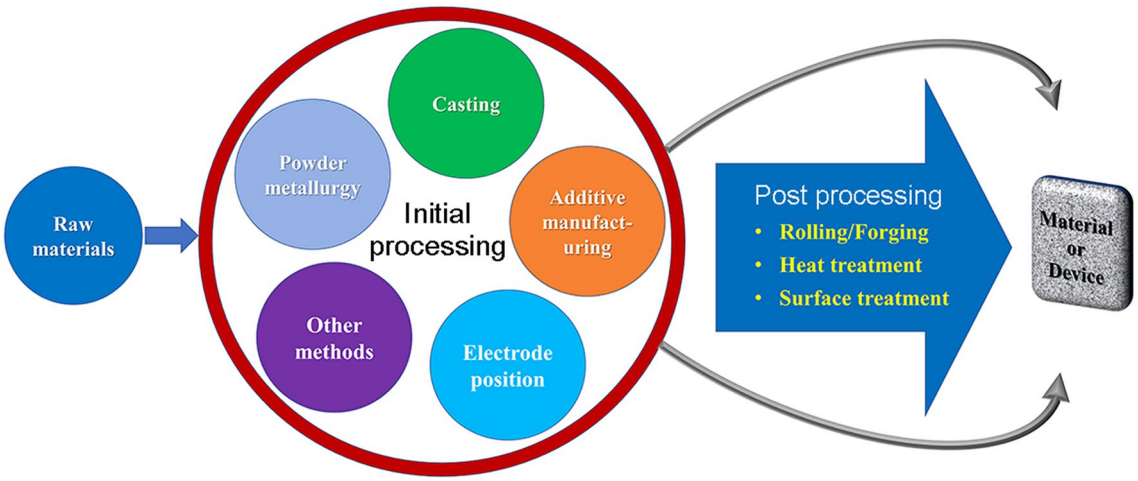

Fig. 4 Manufacturing methods for Fe-based BMs

Table 3 Advantages and disadvantages of various methods for manufacturing Fe-based biodegradable devices

Method	Advantages	Disadvantages
Powder metallurgy	Allows the direct production of relatively complex shapes Materials with tuned properties can be obtained The degradation rate and mechanical characteristics can be varied across a large range by making minor modifications to production parameters A suitable method for developing alloys, composites, and porous materials Ease of tailoring biodegradability by optimising porosity	Difficulties in powder preparation Chances of inhomogeneity during the mixing/milling process leads to poor mechanical properties
Casting	Affordability of alloy component customisation Easy to make complicated geometry	There is a high probability of casting defects as: segregation, blowholes, and shrinkage Post-processing is required after casting Cannot produce Fe-bioceramic composite High-stress shielding
Additive manufacturing	Best method to produce porous scaffolds Ease of tailoring biodegradability by optimising porosity Shape and geometry of pores can be controlled (these decide the osteoconduction and osseointegration Allows implant materials to have mechanical characteristics similar to human bone. (Reduce stress shielding) Accuracy and adaptability	Difficulties in powder preparations
Electroforming	Simple method Does not require complex equipment Less amount of energy consumption	Only thin sections/sheets can be made

Oriňaková et al. 2016). The versatility of the PM process makes it possible to produce components with different shapes and other features from powders. Hermawan et al. (2007, 2008) developed an alloy of Fe–Mn alloys with Mn content varying from 20 to 35% (*b* wt) by PM route and reported that the alloys exhibited a higher degradation rate than that of pure Fe in the physiological environment. They found that Fe–20Mn and Fe–25Mn alloys have multiphase microstructures and those of Fe–30Mn and Fe–35Mn are single-phase microstructures. The multiphase alloys show a higher degradation rate (1.1–1.3 mmpy) than the single-phase alloys (0.4–0.7 mmpy). In addition, the magnetic susceptibility of all alloys was similar to that of the SS316L (Hermawan et al. 2010b). The authors have developed Fe–Mn alloys with the composition of Fe–25 Mn and Fe–35Mn which exhibit an average degradation rate of 0.5 mmpy, which is twice that of the pure Fe (Hermawan et al. 2010c; Hermawan and Mantovani 2013). Wegener et al. (2011) manufactured Fe–C (0.01 and 0.02% by wt of C), Fe–P (0.6 and 1.6% by wt of P), Fe–B (0.6% by wt of B), and Fe–Ag (1.0 and 5.0% by wt of Ag) alloys using PM method with low alloy concentration. All alloys have an almost similar degradation rate in the range of 0.123–0.187 mmpy. The degradation rate of various produced materials is summarised in Table 1, included in "Summary and future prospects". However, cytotoxicity evaluation of the samples showed that all alloys, except Fe–P alloys, were slightly cytotoxic. They concluded that unalloyed steel and Fe–P are good candidates for the load-bearing application (Wang et al. 2017b).

The powder metallurgy technique was also used effectively to develop porous samples. Controlling and fine-tuning the porosity can help in improving the degradation rate and bringing the mechanical properties close to that of human bone (Zhang and Cao, 2015; Dehghan-Manshadi et al. 2019). A porous morphology increases the rate of degradation and reduces the modulus of elasticity of the implant. A modulus of elasticity value close to that of bone will help to avoid the stress shielding reported while using conventional implants (Ridzwan et al. 2007; Mour et al. 2010; Shayesteh Moghaddam et al. 2016; Prasad et al. 2017). In addition, porosity is the desired property in implants because it allows for efficient oxygen and nutrient transfer, promotes osseointegration and vascular invasion. It also enhances bioactivity by increasing the interfacial surface area and improves fixation between the implant and surrounding tissues (Shimko et al. 2005; Wegener et al. 2020).

Mandal et al. (2021) used naphthalene (Naph) as a spacer material to develop multiscale porosity in the Fe–Mn–Cu (Fe–Mn–Cu)-based scaffolds. An interconnected multichannel network of macropore scaffolds with porosities ranging from 42 to 76% was achieved by this route. The scaffolds were developed with 30% (wt) Naph had a minimum ultimate compressive strength of 7.21 MPa, comparable with that of human cancellous bone (UCS of 2–12 MPa). The degradation rate of the scaffold increased after incorporating the porosity and the one with highest porosity (76%) showed an increased degradation rate of 2.71 mmpy. The accelerated degradation rate of the scaffolds has no harmful effects on MG63 cells. The in vivo studies have revealed that increased porosity result in increased osteointegration.

Čapek and Vojtěch (2014) developed porous iron of different porosities using ammonium bicarbonate (NH_4HCO_3) as the spacer material. They reported that the samples had primarily two kinds of pores with dimensions ranging between 250 and 500 µm. The formation of small pores was attributed to low compaction and larger pores were formed by the spacers. The larger pores have greater surface area in accelerating the degradation rate. The samples also exhibited improved biocompatibility and enhanced osseointegration by allowing the body fluid through the pores. The study indicates that proper selection of compaction force, powder grain size and spacer materials in Fe can help in fine-tuning the porosity and mechanical properties of Fe samples. A similar study was conducted by Zhang and Cao (2015) on Fe–35 Mn system with NH_4HCO_3 as a space holder that enhanced the porosity between 25 and 31%. The degradation rate of this porous alloy obtained through electrochemical test is 2–8 mmpy with a uniform mode of corrosion. However, a high fraction of closed pores compared to open pores seems to be detrimental to the permeation of tissues. Oriňáková et al. (2013) used PM process to create the open-cell porosity in the microstructure of carbonyl Fe, Fe–CNT (0.5% by wt of CNT) and Fe–Mg (0.5% by wt of Mg) alloys. The electrochemical studies showed that Fe–Mg degrades at a faster rate compared to Fe and Fe–CNT.

Fabrication of open-cell iron foam using sponge impregnation technique was also explored on various Fe-based systems to improve the permeation of the tissues and increase biodegradation rate (Gorejová et al. 2020; Oriňaková et al. 2020; Liu et al. 2020). Recently, Liu et al. (2020) fabricated open-cell Fe–Mn (53% by wt of Mn) based foam by metal slurry impregnation of polyurethane foam followed by sintering. Using this technique, a microstructure with 85% porosity and pore sizes ranging from 375 to 500 µm were developed. More importantly, the pores seemed to be interconnected, resulting in good bioactivity and mechanical properties close to the bone. The degradation rate of the different Fe–Mn foams varied from 0.4 to 1.0 mmpy compared to 0.33 mmpy for the pure iron.

Attempts were also made to tailor the properties of Fe-based systems by post-processing of components developed by powder metallurgy route. Obayi et al. (2015) studied the rolling impact on the microstructure, mechanical characteristics and degradation of porous Fe. Compared to straight rolled samples, cross-rolled samples were recrystallised

at a lower rate due to decreased dislocation density and it showed enhanced mechanical properties. However, the grain boundary corrosion was observed predominantly in unidirectional rolled samples. A similar approach was adopted by Hermawan et al. (2008) to prepare Fe–35 Mn samples from the mixture of Fe and Mn powder through cold pressing followed by sintering. The alloys were subjected to two series of cold-rolling and sintering processes to improve density. The microstructure of the samples showed the evolution of porosity and MnO particles after each cycle. Though the samples were sintered in an inert atmosphere, the air trapped inside the micropores would have resulted in the formation of tiny MnO particles (Gierl-Mayer 2020). These cold-rolled samples exhibited higher degradation rates of 0.44–1.26 mmpy compared to pure annealed Fe of 0.16 mmpy.

Powder metallurgy route was also used for developing metal-matrix composites. Fe/bioceramic composites were developed by many research groups to achieve better biocompatibility and biodegradability (Ulum et al. 2014, 2015; Wang et al. 2017b). Ulum et al. (2014) developed Fe-based composite by incorporating hydroxyapatite (HA), tricalcium phosphate (TCP), and biphasic calcium phosphate (BCP) by mechanical alloying and sintering. Compared with pure Fe, the composites exhibited a decrease in yield and compressive strength. The incorporation of bioceramic into the Fe matrix also improved its degradation rate. In vivo and in vitro studies revealed that the dispersed bioceramic phase in Fe matrix could improve cell viability and proliferation. Heiden et al. (2017) developed Fe–Mn/HA porous composites with two different pore diameters of 50 µm and 300 µm as shown in Fig. 5. The Fe–Mn powder was blended with NaCl and HA (average particle of 150 µm) and compressed uniaxially before sintering at 700 °C in an inert environment. The pellets were then immersed in DI water to completely leach NaCl before re-sintering at 1200 °C. The incorporation of HA in the Fe–Mn matrix resulted in the formation of $Ca_2Mn_7O_{14}$ during sintering. The porous morphology increased the degradation rates of Fe–Mn to 0.79 mmpy compared to conventional microstructure (0.24 mmpy). Among the two, those samples of 300 µm pore size degraded at a rate of 0.82 mmpy which was found more favourable for cell adhesion, proliferation, and biomineralisation of bone-like apatite. It possessed better mechanical characteristics than those samples of 50 µm pore size, which degraded rapidly during immersion test. Similarly, Dehestani et al. (2016) prepared Fe–HA composite through powder metallurgy with

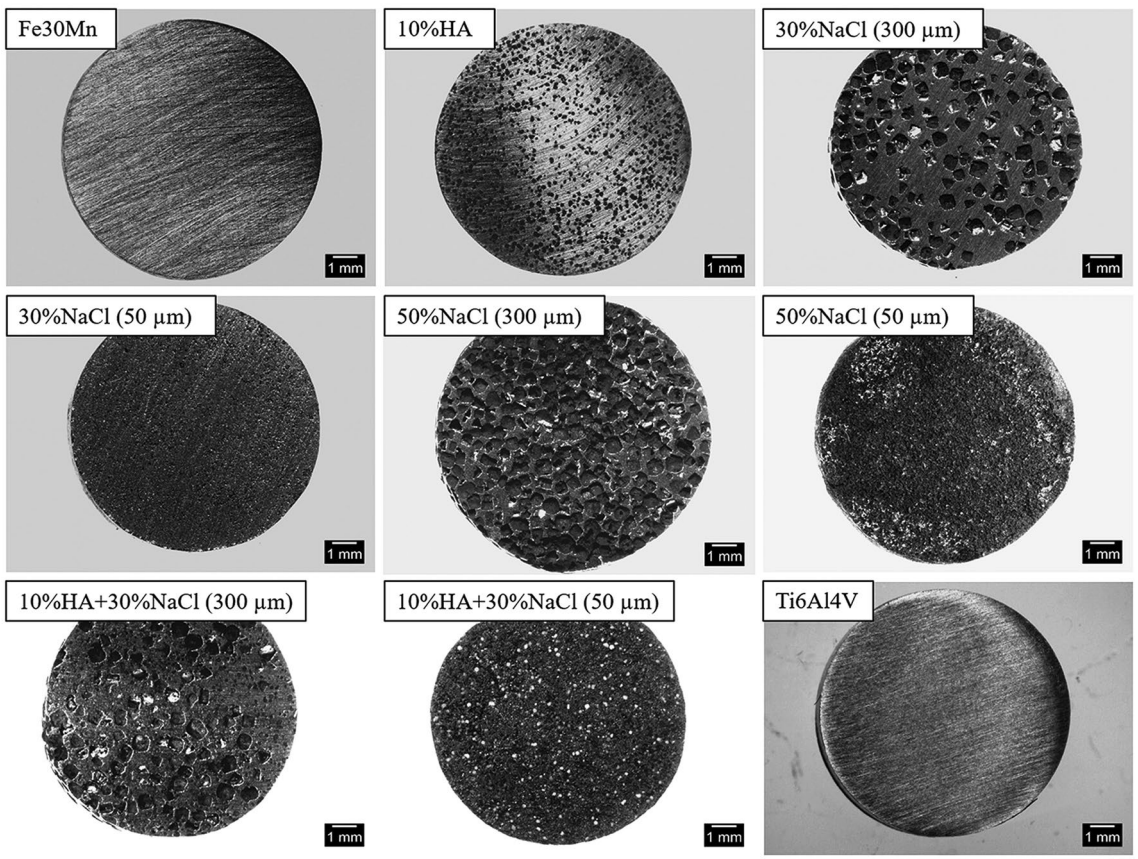

Fig. 5 Optical micrograph of Fe–30Mn, Fe–30Mn–10HA alloy with different porosity developed using NaCl of different size and composition as spacer material (Adapted with permission from WILEY (Heiden et al. 2017))

varying compositions of HA particles having three different classes of particle size: < 1 µm, 1–10 µm, and 100–200 µm. The mechanical properties of the composite decreased with increasing the HA content and lower size of HA particles. When 2.5% (by wt) of HA is added, the values of yield strength and tensile strength of all samples are reduced to half the value for pure Fe. This reduction may be attributed to the formation of dislocation and deformity at the interface of the HA particle and Fe matrix at the grain boundaries. As the HA content increased to 10% (by wt), a significant reduction in tensile strength from 213 to 33.9 MPa was observed. In vitro corrosion rate of Fe–HA composites was in the range of 0.24–1.03 mmpy which were higher than that of the pure Fe (0.11 mmpy). The rate of corrosion increased with increasing the percentage by weight of HA and decreasing the particle size of HA.

Cheng et al. (2014) produced Fe–Fe_2O_3 composite by Spark plasma sintering (SPS) from Fe–Fe_2O_3 powders having varying the percentage by weight (2, 5, 10, and 50) of Fe_2O_3. The microstructure of the composite had a fine-grained structure. The addition of small amounts of Fe_2O_3 (2 and 5% by wt) significantly increased the yield and compressive strength of the composite, while the yield and ultimate strength were found to be decreased at 50% by wt of Fe_2O_3. In both electrochemical and immersion tests, the composite made from the Fe–5Fe_2O_3 exhibited a higher degradation rate. The in vitro studies state that the composite has no cytotoxicity to ECV304 and L929 cells and showed a low haemolysis rate. Similarly, Fe–Au and Fe–Ag composites were made by SPS with different weight percentages of Au and Ag which showed enhanced mechanical properties due to smaller grain size. In the immersion test, the composite degraded nearly 40% faster than the pure Fe (Huang et al. 2016a).

Casting

Casting of Fe-based biodegradable alloys is preferred over other techniques as it helps making intricate shapes and provides better options to alter the composition of alloys. Cheng et al. (2013), studied the feasibility of as-cast pure Fe, Mn, Mg, Zn and W for degradable implant application. It is reported that Mg, Zn and Fe exhibit good biocompatibility, hemocompatibility and cytocompatibility towards L929 and ECV304 cells. However, defects such as segregation, blow holes and shrinkages necessitated post-processing such as extrusion, rolling and forging of these as-cast metals to modify the microstructure, mechanical and corrosion properties of the cast alloy He et al. (2016a). Studies show that cast alloys have shown a degradation rate ranging from 0.105 to 0.29 mmpy (Table 1).

Liu and Zheng (2011) developed binary alloys by incorporating 3% (by wt) Mn/Co/Al/W/Sn/B/C/S into Fe. The addition of Mn, Co, Al, W, and B significantly reduced the degradation rate by 50–75%, whereas adding C and S did not significantly affect the degradation rate in dynamic testing. The yield strength of the alloy dropped considerably with the addition of Sn, while Mn, Co, W, B, C and S have slightly enhanced the strength characteristics of the rolled alloys; these elements have further enhanced the gap between yield and ultimate strength of Fe. Except for Fe–Mn alloy, there was no exceptional cytotoxicity to the ECV304 cells in the extracts of Fe–Co/Al/W/S/B/C/S binary alloys. However, the viability of L929 cells and VSMCs decreased by 10–15% of those extracts. All alloys exhibited a haemolysis percentage of less than 5%. The authors also developed a ternary alloy of Fe with 30% (by wt) Mn and 6% (by wt) Si, which consisted of fine grains of martensite and austenite. The alloy exhibited a higher degradation rate than those of pure Fe and Fe–Mn alloy in the electrochemical corrosion test due to the presents of martensite and austenite phases in the microstructure. The Fe–30Mn–6Si extract exhibited reduced cell viability of 40–50% on ECV304 during the initial period due to the higher ion release. After 2 days, they found that there was an improvement in the viability (60%). However, the viability of VSMC cells was decreased to nearly 30% (Liu et al. 2011).

Schinhammer et al. (2010, 2013), and Moszner et al. (2011), cast Fe–10Mn–1Pd alloys and subjected the same to heat-treatment processes such as recrystallisation and precipitation to improve the microstructural and degradation properties. The alloy was heated to 1250 °C in an inert environment for 12 h, quenched in water, and aged isothermally for 11 days at temperatures below 500 °C. The heat-treated alloy exhibited an increase of 60% in degradation rate compared to pure Fe. During the heat treatment, the Pd-rich precipitate was formed, which prevented the recrystallisation and induced a solute drag effect on the movement of dislocations. Thus, the precipitate helped improve the mechanical properties such as hardness and yield strength. Obayi et al. (2015) studied the effect of the cold-rolling and annealing on the microstructure of as-cast pure Fe. The annealed samples show a slight decrease in the corrosion rate in electrochemical and static immersion tests. The authors have explained the reduction in corrosion rate based on grain size and its distribution. During the annealing process, the average grain size of the sample has increased from 16.5 ± 5 to 19.6 ± 6 µm. The samples with highest average grain size and broad distribution exhibited a higher corrosion rate than those with a smaller average grain size with narrow distribution. The presence of defects and imperfections in the alloy is the most significant factor contributing to the increase

in corrosion rate. The annealing process reduces the flaw density, which reduces the degradation of the material.

Additive manufacturing

The progress in additive manufacturing (AM) technologies has produced unparalleled opportunities to develop porous metallic orthopaedic implants materials with bone regeneration capabilities (Murr et al. 2010; Zadpoor and Malda 2017; Jiang et al. 2021). Different additive manufacturing processes have been adopted to produce the porous degradable Fe-based implants with desired mechanical properties. Chou et al. (2013), developed a Fe–30Mn scaffold with 36.3% open porosity using an ink-jet 3D printing technique. The mechanical properties of the 3D-printed scaffold were similar to that of the human bone. The scaffold exhibited a degradation rate of 0.73 mmpy, which is a promising rate for Fe-based degradable implant application. The authors also reported good cytocompatibility with extensive cell infiltration through the pores during in vitro pre-osteoblast cell viability experiments.

Recent investigations have shown that orthopaedic implants need high porosity and permeability to accommodate nutrient perfusion and good cell viability (Nune et al. 2017). The large pore size leads to weaker mechanical property and low seeding efficiency (Sobral et al. 2011). Li et al. (2018), designed and developed a topologically ordered, highly porous Fe scaffold using the Direct Metal Printing (DMP) technique. In the electrochemical corrosion test, the scaffold structure showed approximately 12 times higher degradation rate than that of pure Fe. The mechanical properties of the scaffold were reduced by nearly 7% after in vitro biodegradation for 28 days in the simulated body fluid, and the scaffold lost its weight by 3.1%. The improved degradation rate was attributed to the porous and topological design of the scaffold. The direct static cell culture study of the scaffold with MG-63 cells exhibited instant cytotoxicity. In the direct culturing of cells on the surface of an iron sample, the local Fe ion concentration can be significantly higher. In addition, AM iron samples with fine grain structures degrade more rapidly and release a greater amount of Fe ions. The increased concentration of Fe ions can develop highly reactive oxygen species such as hydroxyl and superoxide radicals, which are extremely toxic due to their ability to react rapidly with the majority of molecules found in living cells. However, the ISO 10993 indirect test showed a sensible cytocompatibility in in vitro assays for 72 h.

A 3D binder jet printing is another additive manufacturing technique that can be used to create porous Fe-based biodegradable materials (Hong et al. 2016; Yang et al. 2018). Hong et al. (2016) used the technique to develop porous scaffolds using Fe–Mn powder blended with Ca/Mg. The 3D-printed Fe–Mn, and Fe–Mn–1Ca scaffolds had 39.3% and 52.9% porosity and ultimate compressive strength (UCS) values of 228 and 296 MPa, respectively (Morgan et al. 2018). The alloy also exhibited an approximately 12 times higher degradation rate than sintered pellets of the same alloys. In the immersion test, the scaffold containing Ca degrades three times more than the 3D-printed Fe–Mn scaffold and both exhibited better biocompatibility towards MC3T3 cells. Yang et al. (2018) also developed a Fe scaffold by the same method having similar structural porosity and relatively closer mechanical properties (UCS ~ 140 MPa) to that of human bones with good cytocompatibility. Recently Putra et al. (2021), developed porous iron scaffolds through an extrusion-based 3D printing method for degradable orthopaedic implant application. The mechanical properties of the scaffolds (Elastic modulus = 0.6 GPa) were comparable to those of human trabecular bone. After 28 days in vitro static immersion in SBF, the scaffold lost 7% of its mass and slightly increased its elastic modulus due to the formation of degradation products on the surface. However, the scaffold displayed a significant level of cytotoxicity when preosteoblasts were cultured directly on the scaffold.

Carluccio et al. (2020), used selective laser melting (SLM) to prepare Fe–35Mn scaffold as shown in Fig. 6. As a result of the alloying with Mn the degradation rate was five times greater than that of pure Fe, with a value of 0.42 ± 0.03 mmpy. The in vitro studies showed improvement in biodegradation rate without any cytotoxicity towards MC3T3-E1 cells. The cells exhibited good adhesion as well as proliferation on the surface of the scaffold. In vivo experiments conducted for four weeks confirmed new bone matrix development integrated with the implant surface.

SLM technology was used successfully by Shuai et al. (2019c) to create a porous Fe–Mn scaffold. Structural homogeneity and high porosity in the scaffolds demonstrated the accuracy and adaptability of SLM in the fabrication of metal bone implants. Due to the quick solidification impact of SLM, Mn predominantly dissolved in Fe matrix and generated high Mn solid solution, including martensitic and austenitic phases, in the Fe matrix. A more refined and uniform microstructure was produced by the laser quick solidification process as well. The mechanical characteristics of the Fe–Mn scaffold were found to be acceptable for load-bearing applications. Faster and more accurate degradation rates were found in the Fe–Mn scaffold compared to a Fe scaffold. In vitro cell culture studies confirmed that the scaffolds were cytocompatible with good cell proliferation. Traverson et al. (2018), Li et al. (2019b) and Huang et al. (2021) also reported similar results for Fe implants developed through SLM.

Jiang et al. (2021), used an additive manufacturing process called fused filament fabrication (FFF) to make a polylactic acid (PLA)/Fe composite scaffold to investigate how it interacts with bone marrow cells. The composite

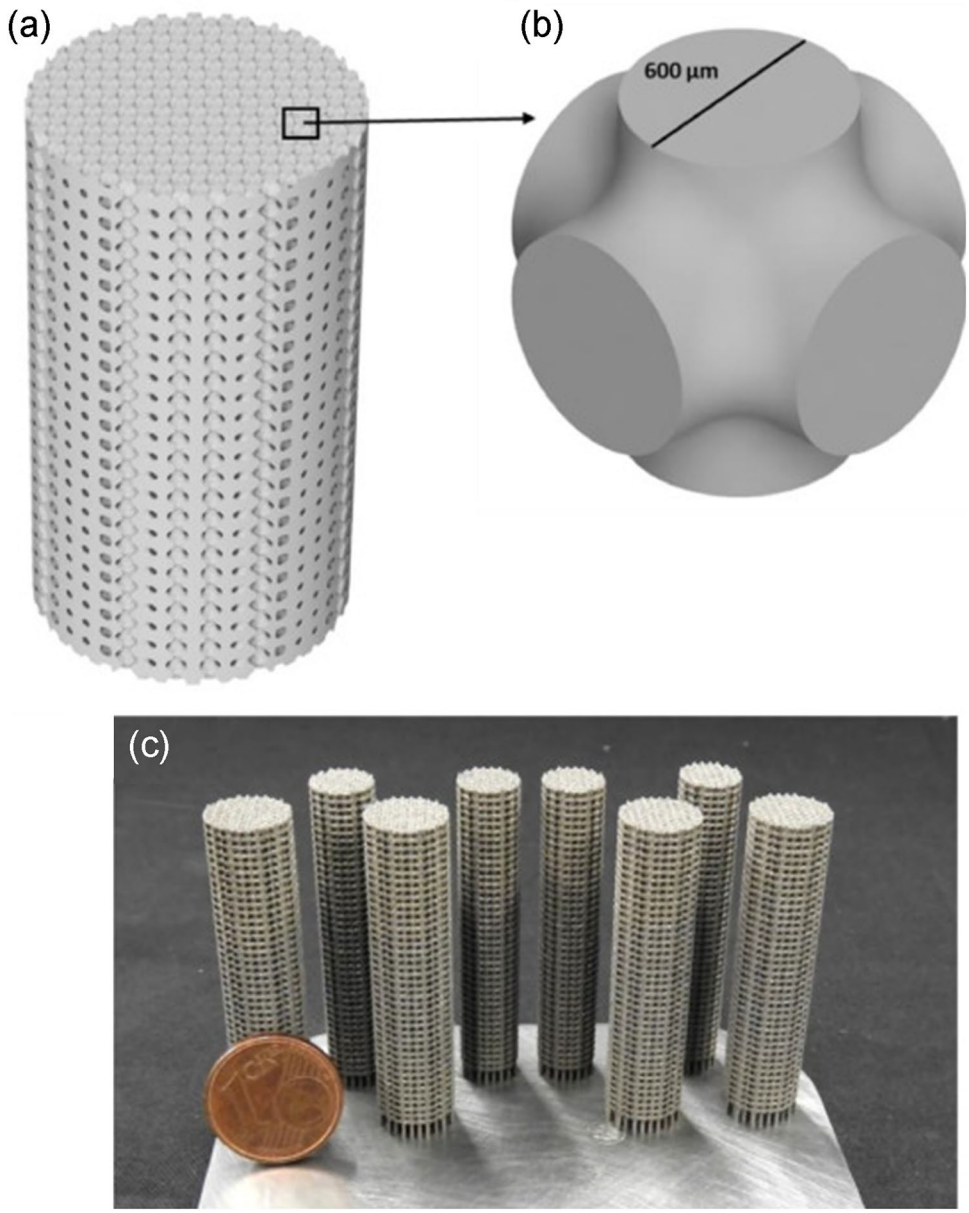

Fig. 6 Details of scaffold design: **a** CAD of the scaffold, **b** repeating unit cell, **c** as manufactured scaffold. (Adapted with permission of Elsevier (Carluccio et al. 2020))

had about 15% more strut width, 8% less pore size, and less surface roughness than the PLA scaffold. PLA/Fe composite had exhibited a good hydrophilic wetting behaviour, which led to better cell interaction and better cytocompatibility. Paul et al. (2022) developed Fe–30Mn–1C–0.02S alloy through laser powder bed fusion (LPBF) and the impact of ion release on cell-materials interaction was investigated. The samples were pre-conditioned in cell culture media for 2 h and 7 and 28 days. The cell adhesion seems unaffected by pre-conditioned surfaces during the initial period. Human umbilical vein endothelial cells (HUVECs) survived for up to 14 days on all three modified surfaces but were able to cope better with the degrading sample after 7 and 28 days of preconditioning. Thus, the authors asserted that the Fe–30Mn–1C–0.02S alloy produced using LPBF demonstrated improved in vitro biocompatibility and that in vivo application is feasible.

Other methods

Advanced techniques can also be adopted after the conventional production methods in developing Fe-based materials to obtain desired and unique properties. Electroforming is one such technique successful used by Moravej et al. (2010a). A thin (~ 100 µm thick) foil of Fe was developed on the surface of Ti6Al4V alloy through electroforming technique. The electroformed Fe (E-Fe) was then separated from the substrate and annealed in an inert atmosphere. The

texture and morphology of the pure electroformed Fe varied significantly with the process parameters, especially the current density. Annealing lowered the strength of the electroformed Fe and enhanced elongation due to the recrystallisation. The E-Fe showed a higher degradation rate value of 0.85 mmpy compared to that of the pure Fe. However, the annealing process brought down the corrosion rate to 0.51 mmpy. The high degradation rate before annealing was attributed to internal stress, strained grains and defects in the as electroformed state. In another study, the authors investigated the effect of thermomechanical treatment on the in vitro biodegradation behaviour and cytocompatibility of E-Fe. Both static and dynamic immersion experiments proved that the degradation of E-Fe is high without the thermomechanical treatment. In addition, E-Fe exhibited good biocompatibility on rat SMCs with enhanced cell proliferation (Moravej et al. 2010b).

He et al. (2019) used a template-assisted electrodeposition method to make 3D porous Fe scaffolds with interconnecting pores. Electrodeposition duration was tuned to control the diameter of the skeletons. The 143 µm diameter scaffolds had a porosity of more than 90% with an average pore size of 345 µm, and mechanical characteristics comparable to that of human bone. Electrochemical deposition of strontium-incorporated octacalcium phosphate (Sr–OCP) with a Sr/(Sr + Ca) ratio of 5% is performed on Fe as shown in Fig. 7 Sr–OCP nanowhiskers with a diameter of 300 nm and a length of 30 µm were deposited with Sr–OCP. The degradation studies revealed that Sr–OCP deposits could efficiently limit the release rate of the Fe ions to ~1.79 mg L^{-1} day^{-1}, which is considered safe for the human body. Cell viability of the MC3T3E1 and MG-63 cells improved to 80% and 100%, respectively, after 24 h of incubation with Sr–OCP-coated Fe scaffolds compared to negative controls. Sr–OCP deposits have been shown to enhance cell adherence in a direct contact cytotoxicity study (He et al. 2019).

Moravej et al. (2011) investigated the influence of current density on microstructure and biodegradability of pure iron Fe developed on Ti surface by electrodeposition method. Four different current densities (1, 2, 5, and 10 A dm^{-2}) were used to electrodeposit iron onto a substrate. It was found that the current density considerably influences the texture, grain size, and grain shape, thereby influencing the material's degradation behaviour. In electrochemical corrosion test, the order of corrosion rate is found to be Fe-2 < Fe-10 < Fe-1 < Fe-5. However, in the immersion test conducted over a period of 14 days, all samples showed a uniform degradation, and there was no significant difference in the degradation rate. A similar degradation rate was explained based on the passivation layer formed on the Fe surface. The authors suggested that the development of electroformed Fe would be more suitable for degradable implant application due to micro pits, which enhance the overall degradation rate.

Jurgeleit et al. (2015, 2016) used magnetron sputtering and UV lithography for developing Au sputtered Fe multilayered foils. The process was tuned to provide a microstructure with Au incorporated between the Fe layers. Three different samples with Au content 0.3, 1 and 2.5% were developed in this work. The introduction of Au enhanced the degradation rate of the foils significantly. It is reported that the samples with 1% at Au exhibit the best compromise between low Au content, mechanical properties and degradation rate. The authors suggested that the precision of this method can help to fabricate devices with a gradient in the microstructure composition. Using this approach, the degradation rate during the initial implantation period can be slowed down to maintain mechanical integrity and promote better implant-tissue interaction. Such a system can be achieved by fine-tuning the process to incorporate a lesser amount of gold on the surface compared to the core of the implant.

Metallurgical and surface modifications for developing Fe-based degradable implants

In addition to the conventional and advanced manufacturing methods discussed in the previous section, various metallurgical and surface modification techniques are also attempted to tailor the degradation behaviour of Fe-based alloys. As shown in Fig. 8, these techniques can be grouped into alloying, microstructure modification, surface modification and morphological modifications. Many researchers have attempted to exploit the difference in electrochemical potential to improve the degradation rate of Fe-based systems by alloying them with more noble elements such as Mn, Au and Ag. The microstructure modification techniques have mainly focussed on developing multiphase microstructure. Such a microstructure is expected to degrade faster than a single-phase alloy. The surface modifications techniques include methods such as coatings for stability during the initial period of implantation, impregnation of noble metals on the surface to create micro-galvanic cells, surface conversions by chemical processing, etc. Improving the surface area by developing porous morphology is also explored as one of the techniques for increasing the degradation rate.

Alloying

Alloying is one of the prominent methods for enhancing the degradation characteristics of Fe. Hermawan et al. (2007, 2008), investigated the feasibility of making degradable Fe alloy by incorporating Mn as the alloying element. Due to

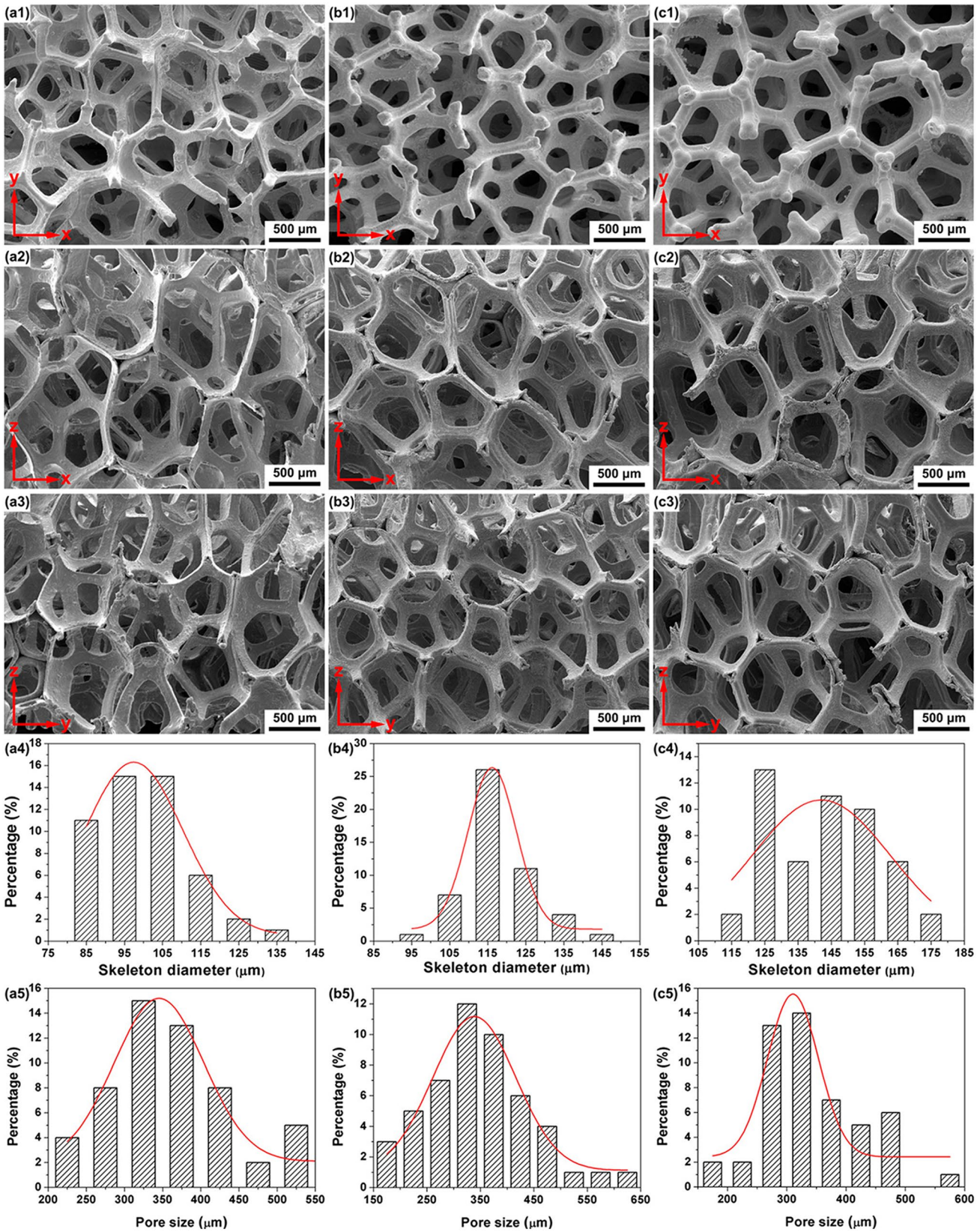

Fig. 7. 3D porous structures viewed from different directions (**a1–c3**), skeleton diameter (**a4–c4**) and pore size (**a5–c5**) distributions of iron scaffolds obtained by electrodeposition for 1 h (**a1–a5**), 1.5 h (**b1–b5**), and 2 h (**c1–c5**), respectively. (Adapted with permission of ACS publications (He et al. 2019))

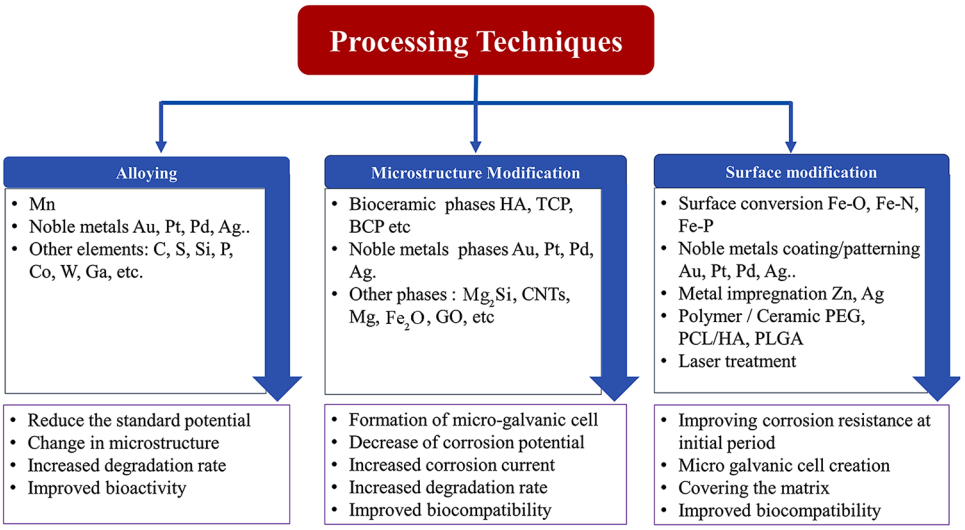

Fig. 8 Summary of processing technique to make Fe-based BMs and their effects

the difference in the standard electrode potential between Fe and Mn forms a less noble Fe–Mn solid solution that degrades much faster than pure Fe. The studies on microstructural, corrosion, magnetic and toxicological characteristics of the Fe–Mn system revealed that Mn could be considered a possible alloying element for improving the degradation rate. Besides, Mn is a trace element essential for the growth, development and regeneration of healthy bone tissues and several enzyme systems (Beattie and Avenell 1992). Thus, Fe–Mn alloy received much interest, and Mn is now considered a preferred alloying element in the Fe matrix for BMs.

The effect of various percentages by weight (20, 25, 30 and 35%) of Mn in Fe was investigated by Hermawan et al. (2010c) and found that the addition of Mn enhances the corrosion rate and starts to decrease as the Mn content increases above 30% (by wt). The work also reported that the inhibition effect on metabolic activities of 3T3 fibroblast cells on Fe–Mn alloy was small compared to pure manganese; Fe–Mn alloy with 35% (by wt). Mn showed a degradation rate of 1.76 mmpy, which is much greater than that of pure Fe (0.14 mmpy) (Hermawan et al. 2008). A similar finding is also reported for 3D-printed Fe–30Mn alloy consisting of binary martensitic and austenitic phases (Chou et al. 2013).

Čapek et al. (2016a), developed a Fe alloy with 30% (by wt) of Mn, which exhibited a corrosion rate 20 times that of pure Fe in the potentiodynamic polarisation (PDP) test. However, a reduced degradation rate was reported in the immersion test in SBF due to the passive layer formation. Traverson et al. (2018), inserted as-cast cold drawn Fe–30Mn alloy into the bone of Sprague–Dawley rats to evaluate the in vivo degradation behaviour of the alloy. After 6 months, partial resorption was observed with increased bone cell integration compared to the conventional SS316L. The alloy was found to be biocompatible without any inflammatory reactions on the host. Nevertheless, it is worth noting that large amounts of manganese can create intoxication and neurotoxic effects (Crossgrove and Zheng 2004; Aschner et al. 2007). Drynda et al. (2015), investigated the degradation and biological behaviour of Fe–Mn alloys having low Mn content (0.5 to 6.9% by wt). In vitro degradation rate of the alloy showed promising results. However, there was no significant degradation observed during in vivo studies due to the formation of the phosphate passivation film.

A combination of other alloying elements such as Pd, Ca, Mg and C along with Mn as the principal alloying element was also explored by researchers. Schinhammer et al. (2010), reported that adding a small amount of Pd into the Fe–10Mn alloy can quadruple the degradation rate. The authors suggested that this accelerated degradation was driven by the formation of solid solution and galvanic interaction of the Fe matrix with the finely dispersed Pd-rich intermetallic phase. The authors also studied the Fe–21Mn system with the addition of C and Pd (Fe–21Mn–0.7C and Fe–21Mn–0.7C–1Pd) (Schinhammer et al. 2013). Both alloys exhibited a significant reduction in polarisation resistance (order of 10^2 Ω cm^2) in EIS studies, indicating improved degradation rates. Hong et al. (2016), investigated the effect of Ca and Mg addition on the degradation and biocompatibility of Fe–35Mn alloy. The corrosion current density of Fe–35Mn–1Ca, Fe–35Mn–2Ca, Fe–35Mn–1 Mg and Fe–35Mn–2 Mg alloys was found to be 2.12, 6.36, 5.89 and 9.16 μA.cm^{-2}, respectively, higher than that of Fe–35Mn alloy (1.00 μA cm^{-2}). Silicon (Si) was also used to improve the degradation performance of Fe-based BM. Liu et al. (2011), reported that the addition of 1% (by wt) Si into Fe–30Mn increased the corrosion current density of the alloy by a factor of 2.5 during the PDP test. Xu et al. (2015a) synthesised a series of Fe–28Mn-based alloys incorporating Si up to 8% by arc melting followed by hot forging. The

Fe–28Mn–6Si alloy degraded nearly 80% faster than that of the Fe–Mn alloy. The existence of duplex phases, varying grain sizes and localised pitting on the forged Fe–Mn–Si alloys resulted in the increase in degradation rate. Drevet et al. (2018), revealed that adding 5% Si into Fe–30Mn alloy has improved its degradation rate to 0.80 mmpy. Recently Trincă et al. (2021), evaluated the in vitro and in vivo analysis of FeMnSi and FeMnSiCa alloys. The in vitro electrochemical corrosion behaviour in the Ringer solution showed that the overall corrosion resistance for Ca-containing alloy has been decreased by more than an order of magnitude. The in vivo study on rabbit tibia for 28 days revealed that the presence of Ca improves the degradation rate of alloy and promotes osteoinduction and osteoconduction.

Mandal et al. (2019), investigated the antimicrobial properties of the Cu incorporated Fe–Mn implant. Fe–$(35 - x)$ Mn–xCu ($x = 0, 1, 3, 5, 10$% by wt) compositions were tested for the degradation, cytocompatibility and antimicrobial activities. A six-time higher degradation than that of pure Fe and a remarkable bactericidal effect was also observed for Fe–Mn–Cu systems without affecting its cytocompatibility. Hufenbach et al. (2017), reported that microalloying 0.025% (by wt) of S to Fe–30Mn–1C could increase the degradation rate by 10% of the base alloy. The incorporation of S resulted in the formation of MnS precipitate in the matrix, which affects the corrosion mechanism leading to an increase in the corrosion rate. Cytotoxicity tests performed in vitro on L929 fibroblast cells revealed that microalloying with B and S does not affect cytocompatibility.

Immersion and electrochemical testing have confirmed the rapid degradation of Fe–Ga alloys and decreased corrosion potential compared to pure iron. Wang et al. (2017a) investigated the effect of Ga along with B and Ta on the degradation behaviour of Fe. They considered Fe–19 Ga, (Fe–19 Ga)–2B and (Fe–19 Ga)–0.5(TaC) alloys. The addition of Ga to Fe increased the corrosion rate to 0.48 mmpy, and addition of B further increased it to 0.63 mmpy, while Ta had a comparatively low corrosion rate of 0.33 mmpy. It is worth noticing that all these alloys exhibited a higher corrosion rate than pure Fe (0.13 mmpy). By observing the surface of each sample after immersion in SBF for 28 days, the authors reported that Fe–19 Ga had lost most of its surface compared to the other alloys. The cell culture studies on the same samples showed that MC3T3-E1 cells demonstrated excellent adherence and proliferation on the Fe–Ga alloy surfaces.

Kraus et al. (2014), carried out in vivo study on Fe-based BMs alloys (Fe–10Mn–1Pd and Fe–21Mn–0.7C–1Pd), inserting Fe-based pin into the femoral bone of Sprague–Dawley Rat. After the surgical procedure, the wound displayed mild oedema for 1–2 days and was consistent with the clinical features. Histological findings showed that Fe degradation products were largely Fe^{3+} and comparatively small Fe^{2+} in tissue near implants. There was no inflammation or local toxicity, and no implant-adjacent tissue was damaged due to degradation. Studies by Fântânariu et al. (2015), reveal that Fe–Mn–Si alloy subcutaneous implants were more biocompatible than the tibia implant, though they showed a slow degradation. However, porous Fe–Mn–Si alloy with lower Si content (less than 4% by wt) exhibited a better degradation due to the porous structure (Xu et al. 2015b).

Microstructure modification

The incorporation of second phases into the Fe matrix is another approach for enhancing the degradation rate of Fe composite. These secondary phases act as cathodes in the anodic Fe matrix to form micro-galvanic couplings. These result in lower corrosion potential and increased corrosion current. Noble metal elements such as Au, Pt, Pd and Ag were added to the Fe matrix as the second phase to improve the degradation performance (Huang et al. 2014, 2016a). The noble elements form fine and uniformly distributed intermetallic phases, creating micro-galvanic couples in the iron matrix to give more active sites to the galvanic corrosion (Zheng et al. 2014).

Pd is used to increase the biodegradability of Fe due to its higher nobility (+0.99 V vs. SHE) (Crangle 2006). In addition, Pd can stabilise iron in its non-magnetic austenite state, preferred for implant applications. Pd is miscible with Fe at high temperatures and can be made to precipitate in Fe matrix by a proper heat treatment process (Geurtsen 2002; Nouri and Wen 2021). Schinhammer et al. (2010, 2012, 2013) added 1% (by wt) noble Pd to Fe matrix. In a 28-day immersion test in SBF, the Pd alloying doubled the degradation rate of the Fe–Mn system. The accelerated degradation rate was caused by the uniformly distributed Pd-rich phases, creating micro-galvanic cells in the Fe matrix. In addition, this precipitate strengthens the alloy by reducing the Zener drag effect at the boundary. Ag is another noble metal used to accelerate the degradation of Fe-based implants due to its higher electrochemical potential (+0.800 vs. SHE), biocompatibility, and antibacterial characteristics (Bosetti et al. 2002). An increased degradation rate was exhibited by adding 2% (by wt) of Ag and Pd to Fe. The introduction of Pd did not affect the cytocompatibility, which indicated that Fe-based alloys were cytocompatible as far as the release rate of ions is below tolerance ranges (Čapek et al. 2016b).

Other noble metals such as Pt and Au are employed to accelerate the degradation of Fe. Pt (+1.18 V vs SHE) and Au (+1.69 V vs SHE) have a high electrochemical potential and are biocompatible, making them an ideal secondary phase in Fe matrix for BMs application (Geurtsen 2002; Nouri and Wen 2021). Huang et al. (2014), reported that adding 5% (by wt) of Pd and Pt into the iron matrix

significantly improves the degradation rate for pure iron, particularly for Fe–Pt composites. In the static immersion test, the addition of Pd and Pt increased the degradation rate of Fe by approximately 50% and 100%, respectively. The authors suggested that finely distributed Pd and Pt phases act as cathodic sites, and bulk Fe matrix act as an anode, creating a large number of micro-galvanic couplings and resulting in a higher degradation rate. The addition of Pd and Pt phase in the Fe matrix did not cause any cytotoxicity towards L-929 and ECV304 cells. The author reported similar mechanisms and enhanced degradation for Fe–Au (with 2, 5 percentage by weight of Au) and Fe–Ag (with 2, 5 percentage by weight of Ag) composites during the in vitro immersion test in Hank's solution without any cytotoxic effect on L-929, EA. Hy-926, and VSMC cells (Huang et al. 2016a). Sharipova et al. (2018), developed Fe–5Ag and Fe–10Ag nanocomposites from Fe–Ag_2O powder. Innumerable Fe–Ag nano galvanic cells contributed towards accelerating the degradation rate of developed nanocomposites in saline solution. The increase in the degradation rate was 4 to 20 times higher than that of the similar micro-grain-sized Fe–Ag composites reported by Huang et al. (2016a).

It is also reported that dispersion of soluble bioceramics in Fe matrix can improve the biodegradation rate (Ulum et al. 2014; Montufar et al. 2016; Wang et al. 2017b; Shuai et al. 2019b; Gao et al. 2020). Ulum et al. (2014), reported that the incorporation of 5% (by wt) of hydroxyapatite (HA)/5% (by wt) tricalcium phosphate (TCP)/5% (by wt) biphasic calcium phosphate (BCP-40% (by wt) HA and 60% (by wt) TCP) to Fe matrix (Fig. 9) to achieve and enhanced the degradation rate. In vitro immersion test showed a significant increase in the degradation rate of the composite compared to pure Fe. When tested in SBF for 14 days, the dispersion of HA, TCP, and BCP to Fe matrix increased the degradation rate by 2, 5, and 3 times, respectively. It is also reported that the bioceramic phases increased biocompatibility by 20% when compared to pure Fe. Wang et al. 2017b, prepared a Fe–bioceramic composite with large amount (20–40% by wt) of calcium silicate (Ca_2SiO_4) as a secondary phase. Finely distributed Ca_2SiO_4 bioceramic in Fe matrix has exhibited almost similar compressive and bending strength of human bone and enhanced the degradation when immersed in SBF for 7 days. The addition of 20% (by wt) CS to iron increased the degradation rate by three times, and when increased to 40% (by wt) CS the samples exhibited an eightfold improvement in the degradation rate. Furthermore, compared to pure iron, the composite containing 20% (by wt) CS demonstrated a higher effect in promoting the proliferation of hBMSCs. Reindl et al. (2014), examined the impact of adding different percentages by volume (30, 40 and 50) of β-TCP to a pure Fe matrix on the degradation rate using a long-term in vitro immersion test in 0.9% NaCl solution. After 56 days of immersion, all samples exhibited an increased degradation rate, and composite with 40% by

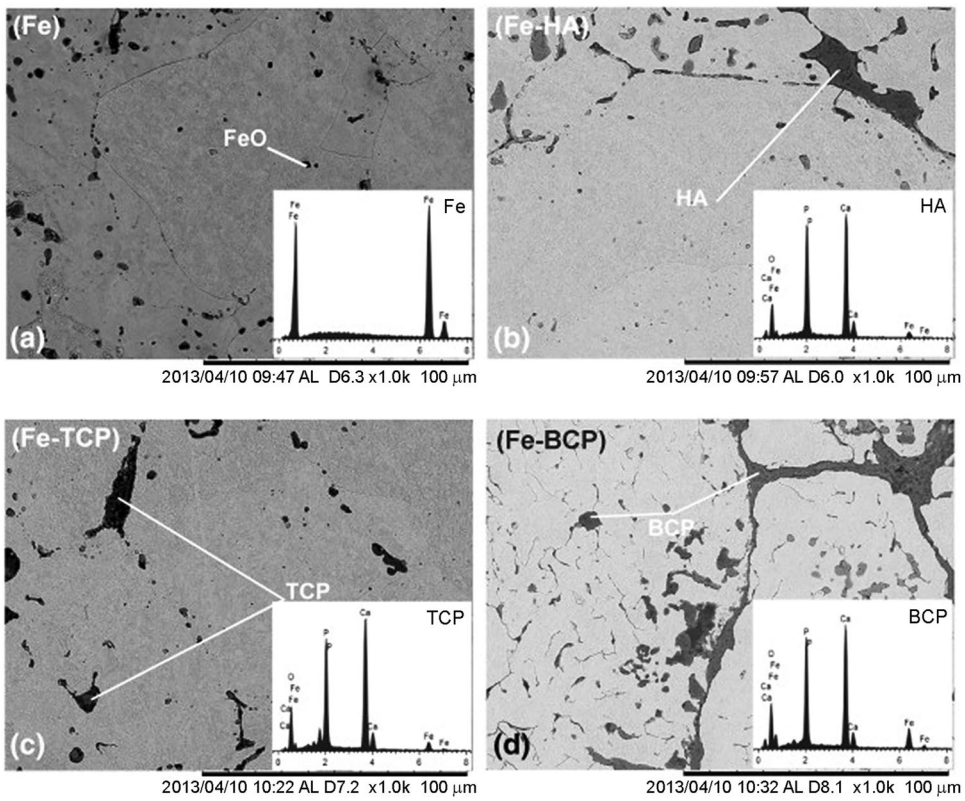

Fig. 9 SEM images and EDS spectra (inset) of **a** pure Fe, **b** Fe–HA, **c** Fe–TCP, and **d** Fe–BCP. (Adapted with permission of Elsevier (Ulum et al. 2014))

vol β-TCP showed remarkable rise of 28% in the degradation rate.

Cheng and Zheng (2013), produced two different composites with W (2 and 5% by wt) and CNT (0.5 and 1% by wt). The electrochemical corrosion test demonstrated that adding W to the Fe matrix increased corrosion by around 10- to 20-fold, although the immersion test revealed no significant increase in degradation rate. However, the addition of CNT to Fe accelerated corrosion by almost 13 times in electrochemical tests and nearly doubled degradation in immersion tests. Both composites were determined to be satisfactory in terms of cytocompatibility and hemocompatibility. The authors also investigated the effect of Fe_2O_3 in Fe matrix for the degradable implant application with various (2, 5, 10 and 50% by wt) of Fe_2O_3 (Cheng et al. 2014). At low concentrations (Fe–2 Fe_2O_3 and Fe–5 Fe_2O_3), a new phase FeO was identified rather than Fe_2O_3, and all compositions increased the degradation rate of Fe. The composite containing 5% Fe_2O_3 degraded more rapidly than the others in electrochemical and immersion tests. Cell culture studies showed that all composites were biocompatible with L929, VSMC, and ECV304 (Cheng et al. 2014). Oriňáková et al. (2013), observed that when 0.5% (by wt) of CNT was added to the Fe-based scaffold, the degradation rate decreased dramatically (twofold that of the pure Fe scaffold) in Hank's solution (8 weeks). However, adding the same amount (0.5% by wt) of Mg greatly enhanced the degradation rate (twofold that of the pure Fe scaffold). Similarly, Sikora-Jasinska et al. (2019) also reported that adding 1% (by wt) Mg_2Si into Fe matrix doubled its degradation performance. A unique corrosion mechanism observed in Fe–Mg_2Si composite in modified Hank's solution is caused by the preferential anodised dissolving of Mg in the Mg_2Si. The corrosion behaviour was explained based on the dissolution of Mg_2Si and the pitting of Fe at the matrix reinforcement interface.

Recently, Zhao et al. (2020), investigated the effect of graphene oxide (GO) in Fe by developing Fe–xGO (x ranging from 0.4% by wt to 1.6% by wt) composites with evenly distributed GO nanoparticles as the second phase. The electrochemical tests showed that E_{corr} values shift to the negative side with an increase in GO content, implying a higher degradation rate. Similarly, in the immersion test, the released iron ion concentrations are 20% higher than those of pure Fe, asserting that Fe–xGO degrades at a faster rate due to the micro-galvanic coupling between the GO and Fe matrix.

Surface modification

Surface modification is a common approach for tailoring the bioactivity, biocompatibility and degradation of BMs. Treatments on the metal surfaces can help in tailoring the bioactivity, resulting in improved osteointegration and hemocompatibility (Gao et al. 2017; Hanas et al. 2018; Ansari 2019; Al-Amin et al. 2020; Oriňaková et al. 2020; Rahim et al. 2021).

Huang et al. (2016b) impregnated Ag ions into the pure iron surface with a metal vapour vacuum arc (MEVVA) technique. A 60-nm-thick layer of Ag_2O and Ag has been observed on the surface with Ag impregnated into the subsurface Fe matrix. This Ag and Ag_2O particles on the surface promoted the degradation rate of the Fe in the electrochemical and immersion test through galvanic corrosion. In electrochemical tests and during the initial period of immersion, the corrosion rate of the Fe doubled due to the Ag implantation on surfaces. While after 15 days of immersion, no substantial difference was seen because the solution eroded the Ag-containing surface and subsurface layer. The cell culture studies using L-929, EA. hy-926, and VSMC cells showed slightly lower viability than the pure Fe though the reduction was within the acceptable range. The authors also studied the effect of Zn implantation on the iron surface using the same procedure and reported a similar result. However, ZnO formed at the surface instead of Zn atoms and a Fe–Zn solid solution formed underneath the ZnO layer (Huang et al. 2016c).

Surface modification by incorporation of noble metals also accelerated the degradation of Fe-based BMs. Cheng et al. (2015), reported that a vacuum sputtered micro-patterned array of Au on the surface of the Fe can effectively enhance its degradation rate. The influence of three different sizes (200×200 μm^2 and 50×50 μm^2) of micro-patterned Au arrays on the degradation of pure iron was investigated. In electrochemical tests, both patterns demonstrated an increased corrosion rate 2.338 and 3.174 g·m^{-2}·d^{-1} compared to pure Fe (0.617 g·m^{-2}·d^{-1}). The authors suggested that the enhanced degradation rate and uniform corrosion behaviour mainly result from the galvanic cell creation between Au disc and Fe. Huang and Zheng (2016), used a similar approach to create a pattern of Pt discs on the iron surface (as shown in Fig. 10). In both electrochemical and immersion tests, the coated Fe degradation rate was nearly three times higher than uncoated Fe. All of the test specimens were non-toxic to EA. hy-926 cells but significantly inhibited VSMCs proliferation. Li et al. (2021), recently demonstrated that a nanometre-thick layer of ZnO can effectively control the degradation of highly interconnected porous Fe. The coating exhibits a significant level of antibacterial activity, and the authors propose that these ZnO-coated porous scaffolds with 3D porous structure could be a potential antibacterial scaffold for bone regeneration and repair.

Wen et al. (2013), modified the surface of Fe foam by electrophoretic deposition of the calcium phosphate/chitosan layer. The coated iron foam shows a better degradation after immersion in (phosphate-buffered saline) PBS and SBF. Yusop et al. (2015), investigated the effect of coating pure porous Fe with poly lactic-co-glycolic acid (PLGA).

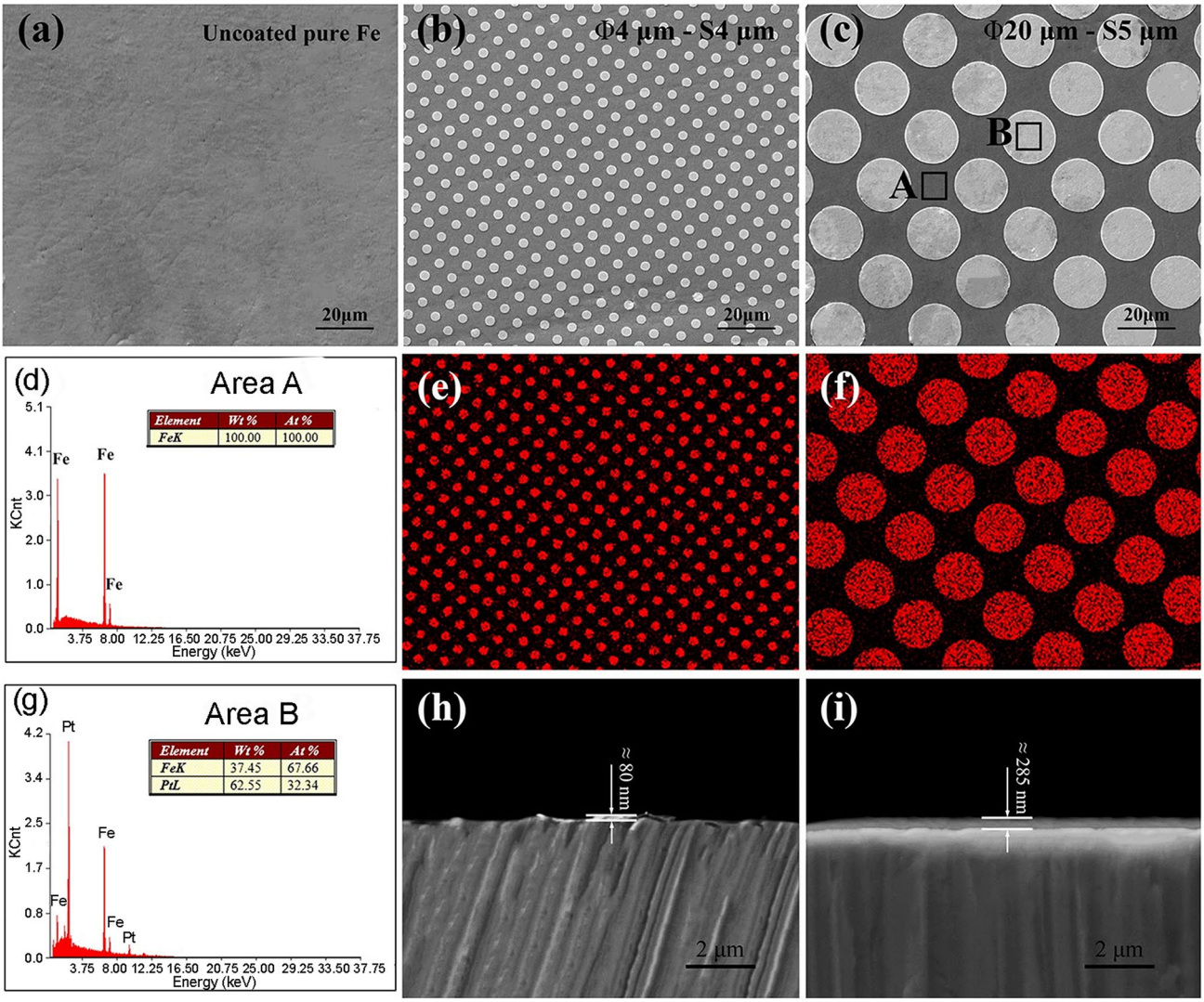

Fig. 10 Surface morphology of the pure iron **a** before and **b** after coated with micro-patterned Pt discs size Φ4 μm × S4 μm and **c** after coated with micro-patterned Pt discs size Φ20 μm × S5 μm (**d**) and (**g**) are energy spectrum analysis related to area A and B, respectively, **e**, **f** are energy spectrum plane scanning analysis of Pt, **h**, **i** are the cross-sections of Φ4 μm × S4 μm and Φ20 μm × S5 μm patterned pure iron, respectively. (Adapted with permission of Springer Nature (Huang and Zheng 2016))

They used the vacuum infiltration method to produce a dense PLGA-filled porous Fe, and the dip-coating method for low-dense PLGA-filled porous Fe. The dense PLGA-filled porous Fe demonstrated a significant improvement in degradation during a four-week immersion test in PBS solution, with a degradation rate of 6.42 mmpy, compared to the low-dense PLGA-filled porous Fe and porous Fe, which show degradation rates of 0.76 and 0.33 mmpy, respectively. The hydrolysis of the polymer coating is the primary factor contributing to the increased degradation rate. As the PLGA hydrolysis proceeds, the pH in the area decreases, facilitating the dissolving of the degradation product and accelerating the degradation reaction. Though the PLGA-coated Fe degrades more rapidly, it had no effect on the cytocompatibility of the human fibroblast cell.

Haverová et al. (2018), studied the effect of poly-ethylene glycol (PEG) coating on the Fe foam surface. The corrosion potential of the coated samples changed to the negative side, resulting in a corrosion rate of 0.53 to 0.70 mmpy, which was much higher than the corrosion rate of uncoated Fe. After 12 weeks of static immersion in SBF, they observed that all coated samples exhibit a weight loss nearly double that of uncoated Fe. The increased rate of iron degradation is due to the interfacial contact between the hydrophilic polymer layer and the Fe surface. The in vitro biocompatibility of PEG-coated Fe foam was investigated by Oriňaková et al. (2019), through indirect and direct cell culture methods

using adult human dermal fibroblast (HDFa) cells. All PEG-coated samples had a viability of greater than 90%, and cell growth was 20–50% greater than that of the pure Fe extract.

According to Qi et al. (2019), the metal-polymer composite coating process is an effective solution for controlled degradation of metals. Polymers such as poly(methyl methacrylate) (PMMA) and polylactic acid (PLA) were coated on Fe to tailor its degradation when subjected to biomimetic conditions. The degradation morphologies of Fe with/without polymer coatings after immersion in Hank's solution are depicted in Fig. 11. The corrosion current density of PLA-coated Fe was nearly three times that of a bare and PMMA-coated Fe. Since PLA can be hydrolysed to form terminal carboxyl groups, the effects of H^+ and lactate ions on the degradation of Fe were also investigated. In addition, forming a passive layer on the iron surface contributes significantly to the slow corrosion rate. As a result, the PLA coating potentially accelerates iron corrosion by enhancing oxygen reduction, taking advantage of the slower release of hydrogen ions and the high permeability of oxygen through the polymer coating during tissue formation. PLA hydrolysis and the polymer coating alleviated deposition of passivated layers which led to an increase in local pH near Fe and resulting in further degradation. Electrochemical and static immersion studies conducted by Hrubovčáková et al. (2017), have shown that coated Fe-foams with PLA degrade more rapidly than non-coated Fe foam. The increased rate of degradation is attributed to the hydrolysis of PLA. A recent study by Gorejová et al. (2020), revealed that varying polymer concentration tends to be an effective way of developing devices with desired degradation behaviours. Huang et al. (2020), coated the Fe–30Mn surface with fibrillar Type I collagen via a spin coating process to improve cell compatibility. The experiments demonstrate that the coated surface improved the osteointegration and cytocompatibility of the implant material.

Apart from the above methods, laser-assisted surface modification was also performed to improve the characteristics of Fe-based BMs. Sun et al. (2021), subjected the degradable Fe–30Mn surface to various degrees of ablation using continuous laser and pulsed laser (nanosecond and femtosecond laser). The nanostructure generated by femtosecond laser gave a greater surface area and raised the corrosion rate of the Fe–30Mn alloy by approximately 40%. They also revealed that the laser-modified Fe–30Mn surfaces can promote biodegradability and biocompatibility for biological applications. According to Hočevar et al. (2017), surface laser treatment of Fe–Mn alloys improves corrosion rates by six times over non-treated Fe–Mn alloys.

Donik et al. (2018), altered the surface topology of a Fe–Mn alloy in a similar manner and investigated corrosion behaviour in Hank's solution using the PDP and EIS tests. The PDP studies showed that the corrosion rate of the polished Fe–Mn alloy was eight times that of an unpolished Fe–Mn alloy. In addition, the EIS studies demonstrated a significant reduction in charge transfer resistance following laser treatment. In both studies, the authors suggested that the higher degradation rate is due to the development of a super hydrophilic surface with the increased surface area

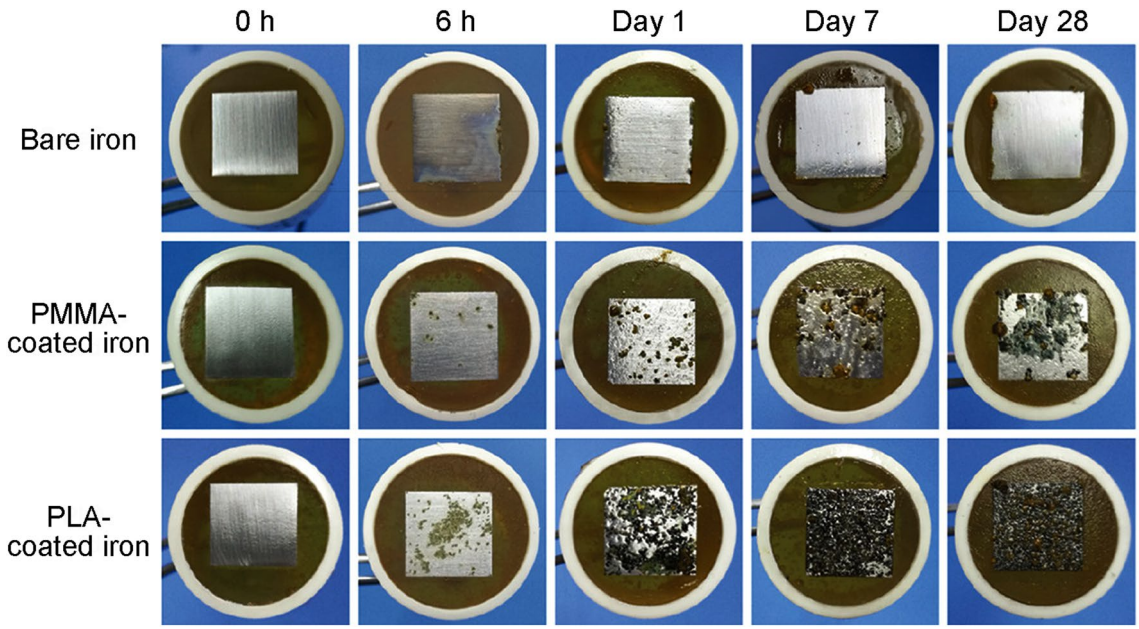

Figure. 11 Degradation morphologies of Fe with and without polymer coatings after immersion in Hank's solution. (Adapted with permission of ACS Publications (Qi et al. 2019))

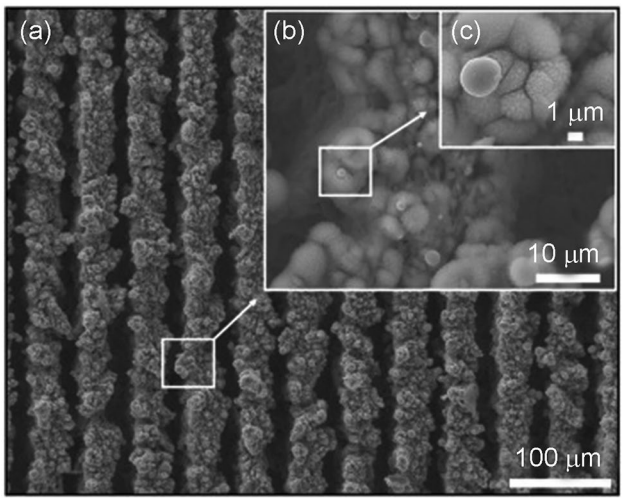

Fig. 12 SEM image of surface topography of Fe–Mn laser-textured sample. (Adapted with permission of Elsevier (Donik et al. 2018))

containing nano-featured oxides formed during laser treatment, as shown in Fig. 12.

It is also important that the enhancement achieved in the degradation should not hinder tissue regeneration. This is crucial during the initial stage of implantation and while using structures with interconnected porosity with small strut thickness. Hence, researchers have attempted to address the premature failure due to enhanced degradation rates by surface modification. Adhilakshmi et al. (2020), found that cathodic electrodeposition of zinc–zinc phosphate–calcium phosphate composite coatings over pure iron is a promising approach for increasing the bioactivity and imparting stability of implant surface during the initial period. The morphological characteristics indicate that plate-like crystals with multi-directional growth and fine pores formed on the coating. During in vitro SBF immersion studies, this bioactive composite surface facilitated the formation of flower-like apatite crystals. The cytocompatibility study shows that the coating

Table 4 Summary of in vitro degradation behaviour of Fe-based BMs developed through various manufacturing and processing methods

Materials	Manufacturing route	Processing method	Degradation medium	Corrosion rate		Yield strength (MPa)
				Electrochemical	Static immersion	
Fe–W (Cheng and Zheng 2013)	Powder metallurgy	–	Hank's solution	1.604–3.025 $gm^{-2}d^{-1}$	0.560–0.663 $gm^{-2}d^{-1}$	180–300
Fe–CNT (Cheng and Zheng, 2013)	Powder metallurgy	–	Hank's solution	2.108–2.419 $gm^{-2}d^{-1}$	0.884–1.028 $gm^{-2}d^{-1}$	200–300
Fe–(2–50)Fe_2O_3 (Cheng et al. 2014)	Powder metallurgy	–	Hank's solution	0.107–2.407 $gm^{-2}d^{-1}$	0.273– 0.668 $gm^{-2}d^{-1}$	–
Fe/P	Powder metallurgy	–	Hank's solution	0.665	–	–
Fe/P–Mn (Oriňaková et al. 2016)	Powder metallurgy	–	Hank's solution	2.761 mmpy	–	–
Fe–2Pd (Čapek et al. 2016b)	Powder metallurgy	–	SBF	0.43 mmpy	0.787 mmpy	127.2
Fe–2Ag (Čapek et al. 2016b)	Powder metallurgy	–	SBF	0.33 mmpy	0.141 mmpy	116.2
Fe–2C (Čapek et al. 2016b)	Powder metallurgy	–	SBF	0.51 mmpy	0.653 mmpy	113.3
Fe–HA (Ulum et al. 2014)	Powder metallurgy	–	SBF	4.776 $gm^{-2}d^{-1}$	1.008 $gm^{-2}d^{-1}$	325
Fe–BCP (Ulum et al. 2014)	Powder metallurgy	–	SBF	4.608 $gm^{-2}d^{-1}$	1.488 $gm^{-2}d^{-1}$	312
Fe–TCP (Ulum et al. 2014)	Powder metallurgy	–	SBF	4.344 $gm^{-2}d^{-1}$	2.16 $gm^{-2}d^{-1}$	312
PLGA-incorporated Fe (Yusop et al. 2015)	Powder metallurgy	–	PBS	–	0.420 mmpy	–
Fe/Mg_2Si (Sikora-Jasinska et al. 2017)	Powder metallurgy	–	Modified Hank's solution	0.27–0.31 mmpy	0.19–0.28 mmpy	290–500
Fe–PE (Gorejová et al. 2020)	Powder metallurgy	–	Modified Hank's solution	0.118–0.598 mmpy	0.148–0.697 mmpy	–
Fe–(20–35)Mn (Heiden et al. 2015)	Powder metallurgy	–	Modified Hank's solution	0.4–1.33 mmpy	–	230–440

Table 4 (continued)

Materials	Manufacturing route	Processing method	Degradation medium	Corrosion rate		Yield strength (MPa)
				Electrochemical	Static immersion	
Porous Fe–30Mn (Dehestani et al. 2017)	Powder Metallurgy	–	SBF	1.36 mmpy	1.18 mmpy	48.2
Fe–30Mn (Dehestani et al. 2017)	Powder metallurgy	Heat treated at 700 °C	SBF	0.29 mmpy	0.24 mmpy	134..2
Fe–30Mn (Dehestani et al. 2017)	Powder metallurgy	Annealed at 900 ^{0}C, quenched	SBF	0.33 mmpy	0.42 mmpy	–
PLGA-coated Fe (Yusop et al. 2015)	Powder metallurgy	Surface coating	PBS	–	0.760 mmpy	–
Pure Fe (Cheng et al. 2013)	Casting	–	0.9% NaCl	–	0.008 mmpy	–
Pure Fe (Cheng et al. 2013)	Casting	–	Hank's solution	–	0.105 mmpy	–
Pure Fe (Zhu et al. 2009b)	Casting	–	SBF		4.896 $gm^{-2}d^{-1}$	–
Pure Fe (Moravej et al. 2010b)	Casting	Thermomechanical treated	Hank's solution		0.14 mmpy	–
Pure Fe (Moravej et al. 2010b)	Casting	Annealed at 550 °C	Modified Hank's solution	–	0.16 mmpy	–
Pure Fe (Obayi et al. 2015)	Casting	Rolled	Modified Hank's solution	0.209–0.243 mmpy	0.115–0.144 mmpy	–
Fe–20Mn (Chou et al. 2013)	Casting		Osteogenic media	0.9427 mmpy	–	
Fe–20Mn (Čapek et al. 2016a)	Casting	Rolled	Osteogenic media	0.5397 mmpy	–	
Fe–30Mn–6Si (Čapek et al. 2016a)	Casting		Hank's solution	–	0.29 mmpy	177.8
Fe–Co (Liu and Zheng, 2011)	Casting	Rolled	Hank's solution	2.741–3.025 $gm^{-2}d^{-1}$	0.220–0.250 $gm^{-2}d^{-1}$	
Fe–B (Liu and Zheng, 2011)	Casting	Rolled	Hank's solution	2.577–3.741 $gm^{-2}d^{-1}$	0.070–0.142 $gm^{-2}d^{-1}$	
Fe–Al (Liu and Zheng, 2011)	Casting	–	Hank's solution	2.385–3.327 $gm^{-2}d^{-1}$	0.116–0.140 $gm^{-2}d^{-1}$	
Fe–2Pd (Čapek et al. 2017)	Casting	–	SBF	–	0.9 $gm^{-2}d^{-1}$	279.4
Fe (Čapek et al. 2017)	Additive manufacturing (SPS)	–	SBF	–	3.20 $gm^{-2}d^{-1}$	73
Fe–2Pd (Čapek et al. 2017)	Additive manufacturing (SPS)	–	SBF	–	0.3 $gm^{-2}d^{-1}$	845..8
Fe–2Pd (Porous) (Čapek et al. 2017)	Additive manufacturing (SPS)	–	SBF	–	0.8 $gm^{-2}d^{-1}$	14.7
Fe–Mn (Hong et al. 2016)	3D–printed	–	HBSS	0.04 mmpy	–	189
Fe–Mn–1Ca (Hermawan et al. 2010b)	3D–printed	–	HBSS	0.07 mmpy	–	–
Fe–30Mn (Liu et al. 2011)	3D–printed	–	HBSS	0.73 mmpy	–	106
Fe–C (Liu and Zheng, 2011)	–	Rolling	Hank's solution	3.991 $gm^{-2}d^{-1}$	0.231–$gm^{-2}d^{-1}$	–
Fe–S (Liu and Zheng, 2011)	–	Rolling	Hank's solution	3.088 $gm^{-2}d^{-1}$	0.230 $gm^{-2}d^{-1}$	–

Table 4 (continued)

Materials	Manufacturing route	Processing method	Degradation medium	Corrosion rate		Yield strength (MPa)
				Electrochemical	Static immersion	
Fe–21Mn–0.7C–1Pd (Schinhammer et al. 2013)	–	Cold working	SBF	–	0.21 mmpy	–
Fe–βTCP (Reindl et al. 2014)	Powder injection moulding	–	0.9%NaCl	–	0.196 mmpy	–
Fe with Pt disc patterned(Huang and Zheng 2016)	–	Surface sputtering	Hank's solution	4.4285–4.792 $gm^{-2}d^{-1}$	3.456–3.832 $gm^{-2}d^{-1}$	–
Pure Fe (Feng et al. 2013)	–	Nitride	Modified Hank's solution	–	0.225 mmpy	–
Fe with micro-patterned Au array (Cheng et al. 2015)	–	Surface sputtering	Hank's solution	2.338–3.317 $gm^{-2}d^{-1}$	1.134–1.417 $gm^{-2}d^{-1}$	–
Ag ion-implanted Fe (Huang et al. 2016b)	–	Metal vapour vacuum arc technique	Hank's solution	1.01 $gm^{-2}d^{-1}$	0.55 $gm^{-2}d^{-1}$	–
Zn ion-implanted Fe (Huang et al. 2016c)	–	Metal vapour vacuum arc technique	Hank's solution	2.13 $gm^{-2}d^{-1}$	0.60 g $m^{-2}d^{-1}$	–
Pure Fe (Moravej et al. 2010b)	Electroformed	–	Modified Hank's solution	–	0.85 mmpy	–
Pure Fe (Moravej et al. 2010b)	Electroformed	Annealed	Modified Hank's solution	0.51 mmpy	0.4 mmpy	–
Fe/Fe–W scaffold (He et al. 2016b)	Electrodeposition	–	Hank's solution	–	0.149–0.264 $gm^{-2}d^{-1}$	–
Fe–30Mn (Hufenbach et al. 2018)	–	Forged	SBF	18.91 $gm^{-2}d^{-1}$	0.028 mmpy	–
Fe–30Mn–1C (Hufenbach et al. 2018)	–	Forged	SBF	–	0.2 mmpy	373
Fe–Mn (Liu and Zheng, 2011)	–	Rolled	Hank's solution	1.863 $gm^{-2}day^{-1}$	0.028 $gm^{-2}d^{-1}$	–

has an acceptable level of biocompatibility and a significant increase in cell proliferation. Zhu et al. (2009a) considered the premature failure and studied Lanthanum ion implantation at a 40 kV extracted voltage to improve the surface properties and delay the degradation rate of Fe during the initial implantation period. The formation of La_2O_3 on the iron's surface considerably slowed the iron's ion migration away from the surface, lowering the corrosion current density. Similarly, the surface transformed compound layer comprising two iron nitrides shows significant resistance to corrosion in 0.9% NaCl solution (Chen et al. 2008). These protective films delayed the deterioration in the mechanical integrity of the Fe-based BMs due to corrosion during the initial stage of implantation. However, long-term in vivo degradation studies by Feng et al. (2013), and Lin et al. (2016), revealed that the nitriding on the Fe surface had made a significant enhancement in the degradation rate.

Summary and future prospects

The reported works establish the capability of Fe-based systems for biodegradable implants. Nevertheless, no product of this kind has been launched in the global market. The works emphasise that the temporary implants need to exhibit a uniform degradation rate to avoid premature failure. This primarily depends on the degradation mechanism, and the same can be tailored by modifying microstructure and composition. The studies reveal that a proper combination of manufacturing route and processing techniques such as alloying, microstructure modification, and surface modification can help develop Fe-based biomedical materials. The major findings from in vitro and in vivo studies reported so far are summarised in Tables 4 and 5, respectively.

Among the manufacturing routes, powder metallurgy (PM) and casting route are among the predominant

Table 5 Summary in vivo studies of Fe-based materials as for orthopaedic application

Material	Manufacturing route	Processing method	Implant region	In vivo observation
Fe–10Mn–1Pd and Fe–21Mn–0.7C–1Pd (Kraus et al. 2014)	Casting	Solution-heat-treated	Transcortical into the femur of Sprague–Dawley rats	No local toxicity and clinical anomalies have been observed after surgery
Fe30Mn (wire) (Traverson et al. 2018)	Casting	Cold drawn	Femur bone of Sprague–Dawley rats	Mild local inflammatory reaction around the implant interface, and necrotic poorly stained bone in direct contact with the corrosion layer
Fe–(0.5–6.9)Mn (cylindrical plate) (Drynda et al. 2015)	Casting	Forging	Underneath the subcutis lying on the gluteal muscle fascia of mice	No harmful side effect or inflammatory sign after 9 months
Fe–HA/BCP/TCP (Ulum et al. 2014)	Powder metallurgy	–	Below the membrane of the radial forelegs in the medium-proximal region of Indonesian thin-tailed sheep	Good tissue integration and response up to 10 weeks
Fe–HA/BCP/TCP (Ulum et al. 2015)	Powder metallurgy	–	Radial bones of leg Indonesian thin-tailed sheep	Relatively low tissue response; usual dynamic change in blood cell reaction; zero stress effects; relatively low inflammatory cell count
1.5Fe–Mn–Si (Fântânariu et al. 2015)	Casting	–	Subcutaneous/tibia crest of Wistar rats	Implants exhibited excellent compatibility; no localised reactions; no potential adverse reactions were caused at the implant
FeMnSiCa and FeMnSi (parallelepiped shape) (Trincă et al. 2021)	Casting	Annealing	Implanted on the tibial crest of rabbit for 28 days	The FeMnSiCa implant has improved osteoinductive and osteoconductive capacity based on bone histo-morphometry and CT. Retrieved implants showed extensive corrosion on their surfaces, but in FeMnSiCa in a greater degree
Ta-implanted Fe (Lee et al. 2021)	–	Target-ion induced plasma sputtering	Implanted in medullary cavity of rabbit femur for 1–4 months	Ta–Fe nanoparticles improved osteoblast adhesion and distribution on the implant surface. Thus, nano-Ta–Fe implants were found to be less toxic than the conventional bare Fe implants

techniques adopted by the researchers. Open-cell porous Fe-based materials prepared through PM have shown a suitable degradation rate with mechanical properties similar to human bone. However, more studies need to be carried out to optimise the pore morphology to make it similar to that of bone tissue to improve bioactivity and enhance osseointegration. Compared to the powder metallurgically prepared materials, cast ones exhibit higher density and strength.

3D-printing technology is an advanced and innovative method for developing accurate, three-dimensional scaffolding and implants. This method can be effectively used to incorporate noble element in the bulk of Fe, and such a system is expected to exhibit a uniform and accelerated degradation rate. In addition, the 3D-printing method can be customised to each patient's individual needs, thereby enhancing the effectiveness of the curing process. Electroforming, magnetron sputtering and UV lithographic techniques are proposed to have potential scope for manufacturing thin-sectioned implants for specific applications, including bone cages and thin plates.

Among the processing techniques, alloying effectively altered the microstructure and degradation properties of Fe-based material. Mn is the most frequently used alloying element in Fe. Non-traditional alloying elements such as Zn, Si, and Ag have also been incorporated along with Mn. The majority of alloying elements accelerated the degradation rate during in vitro degradation test. Similarly, the addition of noble elements such as Cu, Pt, Pd, and Au has increased the degradation rate through galvanic coupling. The addition of bioactive and biocompatible bioceramics phases also improved osteointegration. However, the toxicity associated with alloying elements in the physiological environment and their mechanisms of elimination/absorption need to be investigated. In fact, there is a lack of understanding on the bioactive behaviour of elements in the body. An in-depth assessment of how the body responds to these new implants is worth investigating.

Several studies focussed on the surface modification of implant materials employing metallic, polymeric and bioceramic materials. In particular, polymeric and apatite coating on porous Fe enhanced the biodegradation and biocompatibility of the materials. Though the surface modification yielded significant improvement in bioactivity, its effect on the mechanical properties needs to be investigated. Future research on biodegradable Fe-based bone implants must concentrate on in vitro cell culture and in vivo experiments to elucidate the bio-interfacial properties. In addition, addressing present limitations in laboratory tests on degradable materials is crucial for correctly forecasting long-term degradation mechanisms.

The development of Fe-based degradable bone implants is anticipated to take a longer period, owing to the complex interactions with the physiological environment. The research must now focus on determining the proper relations between the type of alloying elements, their composition and processing to achieve desired and controlled degradation rate. In the near future, additional multidisciplinary research on various manufacturing and processing technologies is necessary to speed up the process and covert the same to clinical trials.

Author contributions Conceptualisation, methodology, literature survey, formal analysis, data curation, and writing—original draft: VPMR. Conceptualisation, methodology, writing—critical review and editing, and supervision: TH.

Funding No funding was received to assist with the preparation of this manuscript.

Data Deposition Information Data sharing not applicable to this article as no datasets were generated or analysed during the current study.

Declarations

Conflict of interest The authors declare that they have no known competing financial interests or personal relationships that could have appeared to influence the work reported in this paper.

Compliance with ethical standards The authors declare that this work is original and has not been published elsewhere, nor is it currently under consideration for publication elsewhere.

References

Adhilakshmi A, Ravichandran K, Sankara Narayanan TSN (2020) Cathodic electrodeposition of zinc-zinc phosphate-calcium phosphate composite coatings on pure iron for biodegradable implant applications. New J Chem 44:6475–6489. https://doi.org/10.1039/d0nj00991a

Al-Amin M, Abdul Rani AM, Abdu Aliyu AA, Bryant G, Danish M, Ahmad A (2020) Bio-ceramic coatings adhesion and roughness of biomaterials through PM-EDM: a comprehensive review. Mater Manuf Process. https://doi.org/10.1080/10426914.2020.1772483

Ansari M (2019) Bone tissue regeneration: biology, strategies and interface studies. Prog Biomater 8:223–237. https://doi.org/10.1007/S40204-019-00125-Z

Aschner M, Guilarte TR, Schneider JS, Zheng W (2007) Manganese: recent advances in understanding its transport and neurotoxicity. Toxicol Appl Pharmacol 221:131–147. https://doi.org/10.1016/j.taap.2007.03.001

Bauer S, Schmuki P, von der Mark K, Park J (2013) Engineering biocompatible implant surfaces: Part I: materials and surfaces. Prog Mater Sci 58:261–326

Beattie JH, Avenell A (1992) Trace element nutrition and bone metabolism. Nutr Res Rev 5:167–188. https://doi.org/10.1079/nrr19920013

Bosetti M, Massè A, Tobin E, Cannas M (2002) Silver coated materials for external fixation devices: in vitro biocompatibility and

genotoxicity. Biomaterials 23:887–892. https://doi.org/10.1016/S0142-9612(01)00198-3
Brooks DB, Burstein AH, Frankel VH (1970) The biomechanics of torsional fractures. The stress concentration effect of a drill hole. J Bone Joint Surg Am 52:507–514
Čapek J, Vojtěch D (2014) Microstructural and mechanical characteristics of porous iron prepared by powder metallurgy. Mater Sci Eng C 43:494–501. https://doi.org/10.1016/j.msec.2014.06.046
Čapek J, Kubásek J, Vojtěch D, Jablonská E, Lipov J, Ruml T (2016a) Microstructural, mechanical, corrosion and cytotoxicity characterization of the hot forged FeMn30 (% by wt) alloy. Mater Sci Eng C 58:900–908. https://doi.org/10.1016/j.msec.2015.09.049
Čapek J, Stehlíková K, Michalcová A, Msallamová Š, Vojtěch D (2016b) Microstructure, mechanical and corrosion properties of biodegradable powder metallurgical Fe-2 wt% X (X = Pd, Ag and C) alloys. Mater Chem Phys 181:501–511. https://doi.org/10.1016/j.matchemphys.2016.06.087
Čapek J, Msallamová Š, Jablonská E, Lipov J, Vojtěch D (2017) A novel high-strength and highly corrosive biodegradable Fe-Pd alloy: structural, mechanical and in vitro corrosion and cytotoxicity study. Mater Sci Eng C 79:550–562. https://doi.org/10.1016/j.msec.2017.05.100
Carluccio D, Xu C, Venezuela J, Cao Y, Kent D, Bermingham M, Demir AG, Previtali B, Ye Q, Dargusch M (2020) Additively manufactured iron-manganese for biodegradable porous load-bearing bone scaffold applications. Acta Biomater 103:346–360. https://doi.org/10.1016/j.actbio.2019.12.018
Chaturvedi TP (2013) Allergy related to dental implant and its clinical significance. Clin Cosmet Investig Dent 5:57–61
Chen Q, Thouas GA (2015) Metallic implant biomaterials. Mater Sci Eng R Rep 87:1–57
Chen CZ, Shi XH, Zhang PC, Bai B, Leng YX, Huang N (2008) The microstructure and properties of commercial pure iron modified by plasma nitriding. Solid State Ionics 179:971–974. https://doi.org/10.1016/j.ssi.2008.03.019
Cheng J, Zheng YF (2013) In vitro study on newly designed biodegradable Fe-X composites (X = W, CNT) prepared by spark plasma sintering. J Biomed Mater ResPart B Appl Biomater 101:485–497. https://doi.org/10.1002/jbm.b.32783
Cheng J, Liu B, Wu YH, Zheng YF (2013) Comparative invitro study on pure metals (Fe, Mn, Mg, Zn and W) as biodegradable metals. J Mater Sci Technol 29:619–627. https://doi.org/10.1016/j.jmst.2013.03.019
Cheng J, Huang T, Zheng YF (2014) a. Microstructure, mechanical property, biodegradation behavior, and biocompatibility of biodegradable Fe–Fe_2O_3 composites. J Biomed Mater Res Part A 102:2277–2287. https://doi.org/10.1002/jbm.a.34882
Cheng J, Huang T, Zheng YF (2015) Relatively uniform and accelerated degradation of pure iron coated with micro-patterned Au disc arrays. Mater Sci Eng C 48:679–687. https://doi.org/10.1016/j.msec.2014.12.053
Chou DT, Wells D, Hong D, Lee B, Kuhn H, Kumta PN (2013) Novel processing of iron-manganese alloy-based biomaterials by inkjet 3-D printing. Acta Biomater 9:8593–8603. https://doi.org/10.1016/j.actbio.2013.04.016
Crangle J (2006) Ferromagnetism in Pd-rich palladium-iron alloys. Philos Mag 5:335–342. https://doi.org/10.1080/14786436008235850
Crossgrove J, Zheng W (2004) Manganese toxicity upon overexposure. NMR Biomed 17:544–553
Dehestani M, Adolfsson E, Stanciu LA (2016) Mechanical properties and corrosion behavior of powder metallurgy iron-hydroxyapatite composites for biodegradable implant applications. Mater Des 109:556–569. https://doi.org/10.1016/j.matdes.2016.07.092
Dehestani M, Trumble K, Wang H, Wang H, Stanciu LA (2017) Effects of microstructure and heat treatment on mechanical properties and corrosion behavior of powder metallurgy derived Fe–30Mn alloy. Mater Sci Eng A 703:214–226. https://doi.org/10.1016/j.msea.2017.07.054
Dehghan-Manshadi A, StJohn DH, Dargusch MS (2019) Tensile properties and fracture behaviour of biodegradable iron-manganese scaffolds produced by powder sintering. Materials (basel). https://doi.org/10.3390/ma12101572
Donik Č, Kocijan A, Paulin I, Hočevar M, Gregorčič P, Godec M (2018) Improved biodegradability of Fe–Mn alloy after modification of surface chemistry and topography by a laser ablation. Appl Surf Sci 453:383–393. https://doi.org/10.1016/j.apsusc.2018.05.066
Dorozhkin SV (2014) Calcium orthophosphate coatings on magnesium and its biodegradable alloys. Acta Biomater 10:2919–2934. https://doi.org/10.1016/J.ACTBIO.2014.02.026
Drevet R, Zhukova Y, Malikova P, Dubinskiy S, Korotitskiy A, Pustov PS (2018) Martensitic transformations and mechanical and corrosion properties of Fe–Mn–Si alloys for biodegradable medical implants. Metall Mater Trans A Phys Metall Mater Sci 49:1006–1013. https://doi.org/10.1007/s11661-017-4458-2
Drynda A, Hassel T, Bach FW, Peuster M (2015) In vitro and in vivo corrosion properties of new iron-manganese alloys designed for cardiovascular applications. J Biomed Mater Res Part B Appl Biomater 103:649–660. https://doi.org/10.1002/jbm.b.33234
Fântânariu M, Trincă LC, Solcan C, Trofin A, Strungaru S, Şindilar EV, Plăvan G, Stanciu S (2015) A new Fe–Mn–Si alloplastic biomaterial as bone grafting material: in vivo study. Appl Surf Sci 352:129–139. https://doi.org/10.1016/J.APSUSC.2015.04.197
Feng Q, Zhang D, Xin C, Liu X, Lin W, Zhang W, Chen S, Sun K (2013) Characterization and in vivo evaluation of a bio-corrodible nitrided iron stent. J Mater Sci Mater Med 24:713–724. https://doi.org/10.1007/s10856-012-4823-z
Gao C, Peng S, Feng P (2017) Shuai C (2017) Bone biomaterials and interactions with stem cells. Bone Res 51(5):1–33. https://doi.org/10.1038/boneres.2017.59
Gao C, Yao M, Shuai C, Feng P (2020) Peng S (2020) Advances in biocermets for bone implant applications. Bio-Des Manuf 34(3):307–330. https://doi.org/10.1007/S42242-020-00087-3
Garimella A, Awale G, Parai R, Ghosh SB, Bandyopadhyay-Ghosh S (2019) An integrated approach to develop engineered metal composite bone scaffold with controlled degradation. Mater Technol 34:858–866. https://doi.org/10.1080/10667857.2019.1639004
Geurtsen W (2002) Biocompatibility of dental casting alloys. Crit Rev Oral Biol Med 13:71–84. https://doi.org/10.1177/154411130201300108
Gierl-Mayer C (2020) Reactions between ferrous powder compacts and atmospheres during sintering—an overview. Powder Metall 63:237–253. https://doi.org/10.1080/00325899.2020.1810427
Gorejová R, Oriňaková R, Orságová Králová Z, Baláž M, Kupková M, Hrubovčáková M, Haverová L, Džupon M, Oriňak A, Kaľavský F, Kovaľ K (2020) In vitro corrosion behavior of biodegradable iron foams with polymeric coating. Mater (basel, Switzerland) 13:1–17. https://doi.org/10.3390/ma13010184
Hanas T, Sampath Kumar TS, Perumal G, Doble M, Ramakrishna S (2018) Electrospun PCL/HA coated friction stir processed AZ31/HA composites for degradable implant applications. J Mater Process Technol 252:398–406. https://doi.org/10.1016/J.JMATPROTEC.2017.10.009
Haverová L, Oriňaková R, Oriňak A, Gorejová R, Baláž M, Vanýsek P, Kupková M, Hrubovčáková M, Mudroň P, Radoňák J, Králová ZO, Turoňová AM (2018) An in vitro corrosion study of open cell Iron structures with PEG coating for bone replacement applications. Metals (basel) 8:1–21. https://doi.org/10.3390/met8070499

He J, He F, Li D, Liu YL, Liu YY, Ye YJ, Yin DW (2016a) Advances in Fe-based biodegradable metallic materials. RSC Adv. https://doi.org/10.1039/c6ra20594a

He J, He FL, Li DW, Liu YL, Yin DC (2016b) A novel porous Fe/Fe-W alloy scaffold with a double-layer structured skeleton: Preparation, in vitro degradability and biocompatibility. Colloids Surf B Biointerfaces 142:325–333. https://doi.org/10.1016/j.colsurfb.2016.03.002

He J, Ye H, Li Y, Fang J, Mei Q, Lu X, Ren F (2019) Cancellous-bone-like porous iron scaffold coated with strontium incorporated octacalcium phosphate nanowhiskers for bone regeneration. ACS Biomater Sci Eng 5:509–518. https://doi.org/10.1021/acsbiomaterials.8b01188

Heiden M, Walker E, Nauman E, Stanciu L (2015) Evolution of novel bioresorbable iron-manganese implant surfaces and their degradation behaviors in vitro. J Biomed Mater Res Part A 103:185–193. https://doi.org/10.1002/jbm.a.35155

Heiden M, Nauman E, Stanciu L (2017) Bioresorbable Fe–Mn and Fe–Mn–HA materials for orthopedic implantation: enhancing degradation through porosity control. Adv Healthc Mater 6:1700120. https://doi.org/10.1002/ADHM.201700120

Hermawan H (2018) Updates on the research and development of absorbable metals for biomedical applications. Prog Biomater 7:93–110. https://doi.org/10.1007/S40204-018-0091-4

Hermawan H, Mantovani D (2013) Process of prototyping coronary stents from biodegradable Fe–Mn alloys. Acta Biomater 9:8585–8592. https://doi.org/10.1016/j.actbio.2013.04.027

Hermawan H, Dubé D, Mantovani D (2007) Development of degradable Fe–35Mn alloy for biomedical application. Adv Mater Res 15–17:107–112. https://doi.org/10.4028/www.scientific.net/AMR.15-17.107

Hermawan H, Alamdari H, Mantovani D, Dubé D (2008) Iron–manganese: new class of metallic degradable biomaterials prepared by powder metallurgy. Powder Metall 51:38–45. https://doi.org/10.1179/174329008X284868

Hermawan H, Dubé D, Mantovani D (2010a) Degradable metallic biomaterials for cardiovascular applications. Metals for biomedical devices. Elsevier, Oxford, pp 379–404

Hermawan H, Dubé D, Mantovani D (2010b) Degradable metallic biomaterials: design and development of Fe–Mn alloys for stents. J Biomed Mater Res Part A 93:1–11. https://doi.org/10.1002/jbm.a.32224

Hermawan H, Purnama A, Dube D, Couet J, Mantovani D (2010c) Fe–Mn alloys for metallic biodegradable stents: degradation and cell viability studies. Acta Biomater 6:1852–1860. https://doi.org/10.1016/j.actbio.2009.11.025

Hočevar M, Donik Č, Paulin I, Kocijan A, Tehovnik F, Burja J, Gregorčič P, Godec M (2017) Corrosion on polished and laser-textured surfaces of An Fe–Mn biodegradable alloy. Mater Tehnol 51:1037–1041. https://doi.org/10.17222/mit.2017.140

Hong D, Chou DT, Velikokhatnyi OI, Roy A, Lee B, Swink I, Issaev I, Kuhn HA, Kumta PN (2016) Binder-jetting 3D printing and alloy development of new biodegradable Fe-Mn-Ca/Mg alloys. Acta Biomater 45:375–386. https://doi.org/10.1016/j.actbio.2016.08.032

Hrubovčáková M, Kupková M, Džupon M, Giretová M, Medvecký L, Džunda R (2017) Biodegradable polylactic acid and polylactic acid/hydroxyapatite coated iron foams for bone replacement materials. Int J Electrochem Sci 12:11122–11136. https://doi.org/10.20964/2017.12.53

Huang T, Zheng Y (2016) Uniform and accelerated degradation of pure iron patterned by Pt disc arrays. Sci Rep 6:23627. https://doi.org/10.1038/srep23627

Huang T, Cheng J, Zheng YF (2014) In vitro degradation and biocompatibility of Fe-Pd and Fe-Pt composites fabricated by spark plasma sintering. Mater Sci Eng C 35:43–53. https://doi.org/10.1016/j.msec.2013.10.023

Huang T, Cheng J, Bian D, Zheng Y (2016a) Fe-Au and Fe-Ag composites as candidates for biodegradable stent materials. J Biomed Mater Res Part B Appl Biomater 104:225–240. https://doi.org/10.1002/jbm.b.33389

Huang T, Cheng Y, Zheng Y (2016b) In vitro studies on silver implanted pure iron by metal vapor vacuum arc technique. Colloids Surf B Biointerfaces 142:20–29. https://doi.org/10.1016/j.colsurfb.2016.01.065

Huang T, Zheng Y, Han Y (2016c) Accelerating degradation rate of pure iron by zinc ion implantation. Regen Biomater 3:205–215. https://doi.org/10.1093/rb/rbw020

Huang S, Ulloa A, Nauman E, Stanciu L (2020) Collagen coating effects on Fe–Mn bioresorbable alloys. J Orthop Res 38:523–535. https://doi.org/10.1002/JOR.24492

Huang CC, Lam TN, Amalia L, Chen KH, Yang KY, Muslih MR, Singh SS, Tsai PI, Lee YT, Jain J, Lee SY, Lai HJ, Huang WC, Chen SY, Huang EW (2021) Tailoring grain sizes of the biodegradable iron-based alloys by pre-additive manufacturing microalloying. Sci Rep. https://doi.org/10.1038/S41598-021-89022-9

Hufenbach J, Wendrock H, Kochta F, Kühn U, Gebert A (2017) Novel biodegradable Fe-Mn-C-S alloy with superior mechanical and corrosion properties. Mater Lett 186:330–333. https://doi.org/10.1016/j.matlet.2016.10.037

Hufenbach J, Kochta F, Wendrock H, Voß A, Giebeler L, Oswald S, Pilz S, Kühn U, Lode A, Gelinsky M, Gebert A (2018) S and B microalloying of biodegradable Fe-30Mn-1C—effects on microstructure, tensile properties, in vitro degradation and cytotoxicity. Mater Des 142:22–35. https://doi.org/10.1016/j.matdes.2018.01.005

Ito M, Onodera T, Funakoshi T (2015) Metallic biomaterials in orthopedic surgery. Advances in metallic biomaterials. Springer series in biomaterials science and engineering. Springer, Berlin, pp 213–231

Jiang D, Ning F, Wang Y (2021) Additive manufacturing of biodegradable iron-based particle reinforced polylactic acid composite scaffolds for tissue engineering. J Mater Process Technol 289:116952. https://doi.org/10.1016/J.JMATPROTEC.2020.116952

Jurgeleit T, Quandt E, Zamponi C (2015) Magnetron sputtering a new fabrication method of iron based biodegradable implant materials. Adv Mater Sci Eng 2015:1–9. https://doi.org/10.1155/2015/294686

Jurgeleit T, Quandt E, Zamponi C (2016) Mechanical properties and in vitro degradation of sputtered biodegradable Fe–Au foils. Materials (basel) 9:928. https://doi.org/10.3390/ma9110928

Kabir H, Munir K, Wen C, Li Y (2021) Recent research and progress of biodegradable zinc alloys and composites for biomedical applications: biomechanical and biocorrosion perspectives. Bioact Mater 6:836–879. https://doi.org/10.1016/J.BIOACTMAT.2020.09.013

Kirchhoff C, Braunstein V, Kirchhoff S, Sprecher CM, Ockert B, Fischer F, Leidel BA, Biberthaler P (2008) Outcome analysis following removal of locking plate fixation of the proximal humerus. BMC Musculoskelet Disord 9:138. https://doi.org/10.1186/1471-2474-9-138

Kraus T, Moszner F, Fischerauer S, Fiedler M, Martinelli E, Eichler J, Witte F, Willbold E, Schinhammer M, Meischel M, Uggowitzer PJ, Löffler JF, Weinberg A (2014) Biodegradable Fe-based alloys for use in osteosynthesis: outcome of an in vivo study after 52 weeks. Acta Biomater 10:3346–3353. https://doi.org/10.1016/j.actbio.2014.04.007

Kumar S, Khan MA, Muralidharan B (2019) Processing of titanium-based human implant material using wire EDM. Mater Manuf

Process 34:695–700. https://doi.org/10.1080/10426914.2019.1566609
Lee MK, Lee H, Park C, Kang IG, Kim J, Kim HE, Jung HD, Jang TS (2021) Accelerated biodegradation of iron-based implants via tantalum-implanted surface nanostructures. Bioact Mater 10(9):239–250. https://doi.org/10.1016/J.BIOACTMAT.2021.07.003
Leo Kumar SP, Avinash D (2020) Review on effect of Ti-alloy processing techniques on surface-integrity for biomedical application. Mater Manuf Process 35:869–892. https://doi.org/10.1080/10426914.2020.1748195
Lévesque J, Hermawan H, Dubé D, Mantovani D (2008) Design of a pseudo-physiological test bench specific to the development of biodegradable metallic biomaterials. Acta Biomater 4:284–295. https://doi.org/10.1016/j.actbio.2007.09.012
Li Y, Jahr H, Lietaert K, Pavanram P, Yilmaz A, Fockaert LI, Leeflang MA, Pouran B, Gonzalez-Garcia Y, Weinans H, Mol JMC, Zhou J, Zadpoor AA (2018) Additively manufactured biodegradable porous iron. Acta Biomater 77:380–393. https://doi.org/10.1016/j.actbio.2018.07.011
Li C, Guo C, Fitzpatrick V, Ibrahim A, Zwierstra MJ, Hanna P, Lechtig A, Nazarian A, Lin SJ, Kaplan DL (2019a) Design of biodegradable, implantable devices towards clinical translation. Nat Rev Mater 51(5):61–81. https://doi.org/10.1038/s41578-019-0150-z
Li G, Yang H, Zheng Y, Chen XH, Yang JA, Zhu D, Ruan L, Takashima K (2019b) Challenges in the use of zinc and its alloys as biodegradable metals: perspective from biomechanical compatibility. Acta Biomater 97:23–45. https://doi.org/10.1016/J.ACTBIO.2019.07.038
Li Y, Jahr H, Pavanram P, Bobbert FSL, Puggi U, Zhang XY, Pouran B, Leeflang MA, Weinans H, Zhou J, Zadpoor AA (2019c) Additively manufactured functionally graded biodegradable porous iron. Acta Biomater 96:646–661. https://doi.org/10.1016/j.actbio.2019.07.013
Li YL, He J, Ye HX, Zhao CC, Zhu WW, Lu X, Ren FZ (2021) Atomic layer deposition of zinc oxide onto 3D porous iron scaffolds for bone repair: in vitro degradation, antibacterial activity and cytocompatibility evaluation. Rare Met. https://doi.org/10.1007/S12598-021-01852-8/FIGURES/10
Lin WJ, Zhang DY, Zhang G, Sun HT, Qi HP, Chen LP, Liu ZQ, Gao RL, Zheng W (2016) Design and characterization of a novel biocorrodible iron-based drug-eluting coronary scaffold. Mater Des 91:72–79. https://doi.org/10.1016/j.matdes.2015.11.045
Liu B, Zheng YF (2011) Effects of alloying elements (Mn Co, Al, W, Sn, B, C and S) on biodegradability and in vitro biocompatibility of pure iron. Acta Biomater 7:1407–1420. https://doi.org/10.1016/J.ACTBIO.2010.11.001
Liu B, Zheng YF, Ruan L (2011) In vitro investigation of Fe30Mn6Si shape memory alloy as potential biodegradable metallic material. Mater Lett 65:540–543. https://doi.org/10.1016/j.matlet.2010.10.068
Liu P, Zhang D, Dai Y, Lin J, Li Y, Wen C (2020) Microstructure, mechanical properties, degradation behavior, and biocompatibility of porous Fe-Mn alloys fabricated by sponge impregnation and sintering techniques. Acta Biomater 114:485–496. https://doi.org/10.1016/j.actbio.2020.07.048
Loffredo S, Paternoster C, Mantovani D (2018) Iron-based degradable implants. Reference module in biomedical sciences. Elsevier, Oxford, pp 1–12
Mandal S, Ummadi R, Bose M, Balla VK, Roy M (2019) Fe–Mn–Cu alloy as biodegradable material with enhanced antimicrobial properties. Mater Lett 237:323–0327. https://doi.org/10.1016/j.matlet.2018.11.117
Mandal S, Viraj NSK, Roy M (2021) Effects of multiscale porosity and pore interconnectivity on in vitro and in vivo degradation and biocompatibility of Fe–Mn–Cu scaffolds. J Mater Chem B 9:4340–4354. https://doi.org/10.1039/D1TB00641J
Md Yusop AH, Ulum MF, Al Sakkaf A, Hartanto D, Nur H (2021) Insight into the bioabsorption of Fe-based materials and their current developments in bone applications. Biotechnol J. https://doi.org/10.1002/BIOT.202100255
Montufar EB, Horynová M, Casas-Luna M, Diaz-de-la-Torre S, Celko L, Klakurková L, Spotz Z, Diéguez-Trejo G, Fohlerová Z, Dvorak K, Zikmund T, Kaiser J (2016) Spark plasma sintering of load-bearing iron-carbon nanotube-tricalcium phosphate cermets for orthopaedic applications. JOM 68:1134–1142. https://doi.org/10.1007/S11837-015-1806-9/FIGURES/8
Moravej M, Mantovani D (2011) Biodegradable metals for cardiovascular stent application: Interests and new opportunities. Int J Mol Sci 12:4250–4270
Moravej M, Prima F, Fiset M, Mantovani D (2010a) Electroformed iron as new biomaterial for degradable stents: development process and structure-properties relationship. Acta Biomater 6:1726–1735. https://doi.org/10.1016/j.actbio.2010.01.010
Moravej M, Purnama A, Fiset M, Couet J, Mantovani D (2010b) Electroformed pure iron as a new biomaterial for degradable stents: in vitro degradation and preliminary cell viability studies. Acta Biomater 6:1843–1851. https://doi.org/10.1016/j.actbio.2010.01.008
Moravej M, Amira S, Prima F, Rahem A, Fiset M, Mantovani D (2011) Effect of electrodeposition current density on the microstructure and the degradation of electroformed iron for degradable stents. Materials science and engineering B: solid-state materials for advanced technology. Elsevier B.V, Oxford, pp 1812–1822
Morgan EF, Unnikrisnan GU, Hussein AI (2018) Bone mechanical properties in healthy and diseased states. Annu Rev Biomed Eng 20:119. https://doi.org/10.1146/ANNUREV-BIOENG-062117-121139
Mostaed E, Sikora-Jasinska M, Mostaed A, Loffredo S, Demir AG, Previtali B, Mantovani D, Beanland R, Vedani M (2016) Novel Zn-based alloys for biodegradable stent applications: design, development and in vitro degradation. J Mech Behav Biomed Mater 60:581–602. https://doi.org/10.1016/J.JMBBM.2016.03.018
Moszner F, Sologubenko AS, Schinhammer M, Lerchbacher C, Hänzi AC, Leitner H, Uggowitzer PJ, Löffler JF (2011) Precipitation hardening of biodegradable Fe-Mn-Pd alloys. Acta Mater 59:981–991. https://doi.org/10.1016/j.actamat.2010.10.025
Mour M, Das D, Winkler T, Hoenig E, Mielke G, Morlock MM, Schilling AF (2010) Advances in porous biomaterials for dental and orthopaedic applications. Mater 3:2947–2974. https://doi.org/10.3390/MA3052947
Murr LE, Gaytan SM, Medina F, Lopez H, Martinez E, Machado BI, Hernandez DH, Martinez L, Lopez MI, Wicker RB, Bracke J (2010) Next-generation biomedical implants using additive manufacturing of complex, cellular and functional mesh arrays. Philos Trans R Soc A Math Phys Eng Sci 368:1999–2032. https://doi.org/10.1098/rsta.2010.0010
Niinomi M (2008) Metallic biomaterials. J Artif Org 11:105–110. https://doi.org/10.1007/s10047-008-0422-7
Nouri A, Wen C (2021) Noble metal alloys for load-bearing implant applications. Struct Biomater. https://doi.org/10.1016/B978-0-12-818831-6.00003-3
Nune KC, Kumar A, Misra RDK, Li SJ, Hao YL, Yang R (2017) Functional response of osteoblasts in functionally gradient titanium alloy mesh arrays processed by 3D additive manufacturing. Colloids Surf B Biointerfaces 150:78–88. https://doi.org/10.1016/j.colsurfb.2016.09.050
Obayi CS, Tolouei R, Paternoster C, Turgeon S, Okorie BA, Obikwelu DO, Cassar G, Buhagiar J, Mantovani D (2015) Influence of

cross-rolling on the micro-texture and biodegradation of pure iron as biodegradable material for medical implants. Acta Biomater 17:68–77. https://doi.org/10.1016/j.actbio.2015.01.024
Oriňáková R, Oriňák A, Bučková LM, Giretová M, Medveckỳ L, Labbanczová E, Kupková M, Hrubovčáková M, Koval K (2013) Iron based degradable foam structures for potential orthopedic applications. Int J Electrochem Sci 8:12451–12465
Oriňaková R, Oriňak A, Giretová M, Medvecký LU, Kupková M, Hrubovčiáková M, Maskal'Ová I, MacKo J, Kal'Avský F (2016) A study of cytocompatibility and degradation of iron-based biodegradable materials. J Biomater Appl 30:1060–1070. https://doi.org/10.1177/0885328215615459
Oriňaková R, Gorejová R, Macko J, Ori A, Kupková M, Hrubov M, Juraj Š, Smith RM (2019) Evaluation of in vitro biocompatibility of open cell iron structures with PEG coating. Appl Surf Sci 475:515–518. https://doi.org/10.1016/j.apsusc.2019.01.010
Oriňaková R, Gorejová R, Králová ZO, Oriňak A (2020) Surface modifications of biodegradable metallic foams for medical applications. Coatings 10(9):819. https://doi.org/10.3390/coatings10090819
Papanikolaou G, Pantopoulos K (2005) Iron metabolism and toxicity. Toxicol Appl Pharmacol 202:199–211
Paramitha D, Ulum MF, Purnama A, Wicaksono DHB, Noviana D, Hermawan H (2016) Monitoring degradation products and metal ions in vivo. Monitoring and evaluation of biomaterials and their performance in vivo. Elsevier Ltd, Oxford, pp 19–44
Paul B, Lode A, Placht AM, Voß A, Pilz S, Wolff U, Oswald S, Gebert A, Gelinsky M, Hufenbach J (2022) Cell-material interactions in direct contact culture of endothelial cells on biodegradable iron-based stents fabricated by laser powder bed fusion and impact of ion release. ACS Appl Mater Interfaces 14:439–451. https://doi.org/10.1021/acsami.1c21901
Peuster M, Wohlsein P, Brügmann M, Ehlerding M, Seidler K, Fink C, Brauer H, Fischer A, Hausdorf G, Care I (2001) A novel approach to temporary stenting : degradable cardiovascular stents produced from corrodible metal—results 6–18 months after implantation into New Zealand white rabbits. Heart 1000:563–569
Prasad K, Bazaka O, Chua M, Rochford M, Fedrick L, Spoor J, Symes R, Tieppo M, Collins C, Cao A, Markwell D, Ostrikov K, Bazaka K (2017) Metallic biomaterials: current challenges and opportunities. Materials (basel) 10(8):884. https://doi.org/10.3390/MA10080884
Putra NE, Leeflang MA, Minneboo M, Taheri P, Fratila-Apachitei LE, Mol JMC, Zhou J, Zadpoor AA (2021) Extrusion-based 3D printed biodegradable porous iron. Acta Biomater 121:741–756. https://doi.org/10.1016/J.ACTBIO.2020.11.022
Qi Y, Li X, He Y, Zhang D, Ding J (2019) Mechanism of acceleration of iron corrosion by a polylactide coating. ACS Appl Mater Interfaces 11:202–218. https://doi.org/10.1021/ACSAMI.8B17125/SUPPL_FILE/AM8B17125_SI_001.PDF
Rahim SA, Nikhil TT, Joseph MA, Hanas T (2020) In vitro degradation and mechanical behaviour of calcium phosphate coated Mg-Ca alloy. Mater Technol. https://doi.org/10.1080/10667857.2020.1794278
Rahim SA, Muhammad Rabeeh VP, Joseph MA, Hanas T (2021) Does acid pickling of Mg-Ca alloy enhance biomineralization? J Magnes Alloy 9:1028–1038. https://doi.org/10.1016/J.JMA.2020.12.002
Reindl A, Borowsky R, Hein SB, Geis-Gerstorfer J, Imgrund P, Petzoldt F (2014) Degradation behavior of novel Fe/ß-TCP composites produced by powder injection molding for cortical bone replacement. J Mater Sci 49:8234–8243. https://doi.org/10.1007/s10853-014-8532-5
Reith G, Schmitz-Greven V, Hensel KO, Schneider MM, Tinschmann T, Bouillon B, Probst C (2015) Metal implant removal: benefits and drawbacks—a patient survey. BMC Surg 151(15):1–8. https://doi.org/10.1186/S12893-015-0081-6
Ridzwan MIZ, Shuib S, Hassan AY, Shokri AA, Mohammad Ibrahim MN (2007) Problem of stress shielding and improvement to the hip implant designs: a review. J Med Sci 7:460–467. https://doi.org/10.3923/JMS.2007.460.467
Saito H (2014) Metabolism of iron stores. Nagoya J Med Sci 76:235–254
Scarcello E, Lison D (2020) Are Fe-based stenting materials biocompatible? A critical review of in vitro and in vivo studies. J Funct Biomater 11:2
Schinhammer M, Hänzi AC, Löffler JF, Uggowitzer PJ (2010) Design strategy for biodegradable Fe-based alloys for medical applications. Acta Biomater 6:1705–1713. https://doi.org/10.1016/j.actbio.2009.07.039
Schinhammer M, Pecnik CM, Rechberger F, Hänzi AC, Löffler JF, Uggowitzer PJ (2012) Recrystallization behavior, microstructure evolution and mechanical properties of biodegradable Fe-Mn-C(-Pd) TWIP alloys. Acta Mater 60:2746–2756. https://doi.org/10.1016/j.actamat.2012.01.041
Schinhammer M, Steiger P, Moszner F, Löffler JF, Uggowitzer PJ (2013) Degradation performance of biodegradable FeMnC(Pd) alloys. Mater Sci Eng C 33:1882–1893. https://doi.org/10.1016/j.msec.2012.10.013
Seal CK, Vince K, Hodgson MA (2009) Biodegradable surgical implants based on magnesium alloys—a review of current research. IOP Conf Ser Mater Sci Eng 4:012011. https://doi.org/10.1088/1757-899X/4/1/012011
Seiler HG, Sigel H (1988) Handbook on toxicity of inorganic compounds. Marcel Dekker, United States
Sharipova A, Swain SK, Gotman I, Starosvetsky D, Psakhie SG, Unger R, Gutmanas EY (2018) Mechanical, degradation and drug-release behavior of nano-grained Fe-Ag composites for biomedical applications. J Mech Behav Biomed Mater 86:240–249. https://doi.org/10.1016/j.jmbbm.2018.06.037
Shayesteh Moghaddam N, Taheri Andani M, Amerinatanzi A, Shayesteh Moghaddam N, Taheri Andani M, Amerinatanzi A, Haberland C, Huff S, Miller M, Elahinia M, Dean D (2016) Metals for bone implants: safety, design, and efficacy. Biomanuf Rev 11(1):1–16. https://doi.org/10.1007/S40898-016-0001-2
Sheikh Z, Najeeb S, Khurshid Z, Verma V, Rashid H, Glogauer M (2015) Biodegradable materials for bone repair and tissue engineering applications. Materials (basel) 8:5744–5794. https://doi.org/10.3390/ma8095273
Shimko DA, Shimko VF, Sander EA, Dickson KF, Nauman EA (2005) Effect of porosity on the fluid flow characteristics and mechanical properties of tantalum scaffolds. J Biomed Mater Res B Appl Biomater 73:315–324. https://doi.org/10.1002/JBM.B.30229
Shuai C, Li S, Peng S, Feng P, Lai Y, Gao C (2019a) Biodegradable metallic bone implants. Mater Chem Front 3:544–562. https://doi.org/10.1039/C8QM00507A
Shuai C, Li Y, Yang Y, Peng S, Yang W, Qi F, Xiong S, Liang H, Shen L (2019b) Bioceramic enhances the degradation and bioactivity of iron bone implant. Mater Res Express 6:115401. https://doi.org/10.1088/2053-1591/ab45b9
Shuai C, Yang W, Yang Y, Pan H, He C, Qi F, Xie D, Liang H (2019c) Selective laser melted Fe-Mn bone scaffold: microstructure, corrosion behavior and cell response. Mater Res Express. https://doi.org/10.1088/2053-1591/AB62F5
Sikora-Jasinska M, Paternoster C, Mostaed E, Tolouei R, Casati R, Vedani M, Mantovani D (2017) Synthesis, mechanical properties and corrosion behavior of powder metallurgy processed Fe/Mg2Si composites for biodegradable implant applications. Mater

Sci Eng C 81:511–521. https://doi.org/10.1016/j.msec.2017.07.049

Sikora-Jasinska M, Chevallier P, Turgeon S, Paternoster C, Mostaed E, Vedani M, Mantovani D (2019) Understanding the effect of the reinforcement addition on corrosion behavior of Fe/Mg2Si composites for biodegradable implant applications. Mater Chem Phys 223:771–778. https://doi.org/10.1016/j.matchemphys.2018.11.068

Sing NB, Mostavan A, Hamzah E, Mantovani D, Hermawan H (2015) Degradation behavior of biodegradable Fe35Mn alloy stents. J Biomed Mater Res Part B Appl Biomater 103:572–577. https://doi.org/10.1002/JBM.B.33242

Sobral JM, Caridade SG, Sousa RA, Mano JF, Reis RL (2011) Three-dimensional plotted scaffolds with controlled pore size gradients: effect of scaffold geometry on mechanical performance and cell seeding efficiency. Acta Biomater 7:1009–1018. https://doi.org/10.1016/j.actbio.2010.11.003

Sun Y, Chen L, Liu N, Wang H, Liang C (2021) Laser-modified Fe–30Mn surfaces with promoted biodegradability and biocompatibility toward biological applications. J Mater Sci 56:13772–13784. https://doi.org/10.1007/S10853-021-06139-Y/FIGURES/9

Traverson M, Heiden M, Stanciu LA, Nauman EA, Jones-Hall Y, Breur GJ (2018) In vivo evaluation of biodegradability and biocompatibility of Fe30Mn alloy. Vet Comp Orthop Traumatol 31:10–16. https://doi.org/10.3415/VCOT-17-06-0080

Trincă LC, Burtan L, Mareci D, Fernández-Pérez BM, Stoleriu I, Stanciu T, Stanciu S, Solcan C, Izquierdo J, Souto RM (2021) Evaluation of in vitro corrosion resistance and in vivo osseointegration properties of a FeMnSiCa alloy as potential degradable implant biomaterial. Mater Sci Eng C 118:111436. https://doi.org/10.1016/j.msec.2020.111436

Trumbo P, Yates AA, Schlicker S, Poos M (2001) Dietary reference intakes: vitamin A, vitamin K, arsenic, boron, chromium, copper, iodine, iron, manganese, molybdenum, nickel, silicon, vanadium, and zinc. J Am Diet Assoc 101:294–301. https://doi.org/10.1016/S0002-8223(01)00078-5

Ulum MF, Arafat A, Noviana D, Traverson M, Heiden M, Stanciu LA, Nauman EA, Jones-Hall Y, Breur GJ (2014) In vitro and in vivo degradation evaluation of novel iron-bioceramic composites for bone implant applications. Mater Sci Eng C 36:336–344. https://doi.org/10.1016/j.msec.2013.12.022

Ulum MF, Nasution AK, Yusop AH, Arafat A, Kadir MRA, Juniantito V, Noviana D, Hermawan H (2015) Evidences of in vivo bioactivity of Fe-bioceramic composites for temporary bone implants. J Biomed Mater Res Part B Appl Biomater 103:1354–1365. https://doi.org/10.1002/jbm.b.33315

Vojtěch D, Kubásek J, Šerák J, Novák P (2011) Mechanical and corrosion properties of newly developed biodegradable Zn-based alloys for bone fixation. Acta Biomater 7:3515–3522. https://doi.org/10.1016/J.ACTBIO.2011.05.008

Waizy H, Seitz JM, Reifenrath J, Weizbauer A, Bach FW, Meyer-Lindenberg A, Denkena B, Windhagen H (2013) Biodegradable magnesium implants for orthopedic applications. J Mater Sci 48:39–50

Wang H, Zheng Y, Liu J, Jiang C, Li Y (2017a) In vitro corrosion properties and cytocompatibility of Fe-Ga alloys as potential biodegradable metallic materials. Mater Sci Eng C 71:60–66. https://doi.org/10.1016/j.msec.2016.09.086

Wang S, Xu Y, Zhou J, Li H, Chang J, Huan Z (2017b) In vitro degradation and surface bioactivity of iron-matrix composites containing silicate-based bioceramic. Bioact Mater 2:10–18. https://doi.org/10.1016/j.bioactmat.2016.12.001

Wegener B, Sievers B, Utzschneider S, Müller P, Jansson V, Rößler S, Nies B, Stephani G, Kieback B, Quadbeck P (2011) Microstructure, cytotoxicity and corrosion of powder-metallurgical iron alloys for biodegradable bone replacement materials. In: Elsevier BV (ed) Materials science and engineering B: solid-state materials for advanced technology. Elsevier B.V, Oxford, pp 1789–1796

Wegener B, Sichler A, Milz S, Sprecher C, Pieper K, Hermanns W, Jansson V, Nies B, Kieback B, Müller PE, Wegener V, Quadbeck P (2020) Development of a novel biodegradable porous iron-based implant for bone replacement. Sci Rep 10:1–10. https://doi.org/10.1038/s41598-020-66289-y

Wegener B, Behnke M, Milz S, Jansson V, Redlich C, Hermanns W, Birkenmaier C, Pieper K, Weißgärber T, Quadbeck P (2021) Local and systemic inflammation after implantation of a novel iron based porous degradable bone replacement material in sheep model. Sci Rep 111(11):1–11. https://doi.org/10.1038/s41598-021-91296-y

Wen Z, Zhang L, Chen C, Liu Y, Wu C, Dai C (2013) A construction of novel iron-foam-based calcium phosphate/chitosan coating biodegradable scaffold material. Mater Sci Eng C 33:1022–1031. https://doi.org/10.1016/j.msec.2012.10.009

Wong JY, Bronzino JD, Peterson DR (2012) Biomaterials, 1st edn. CRC

Xu Z, Hodgson MA, Cao P (2015a) Microstructure and degradation behavior of forged Fe–Mn–Si alloys. Int J Mod Phys B. https://doi.org/10.1142/S0217979215400147

Xu Z, Hodgson MA, Cao P (2015b) A comparative study of powder metallurgical (PM) and wrought Fe-Mn-Si alloys. Mater Sci Eng A 630:116–124. https://doi.org/10.1016/j.msea.2015.02.021

Yang C, Huan Z, Wang X, Wu C, Chang J (2018) 3D printed Fe scaffolds with HA nanocoating for bone regeneration. ACS Biomater Sci Eng 4:608–616. https://doi.org/10.1021/acsbiomaterials.7b00885

Yang Y, He C, Dianyu E, Yang Y, He C, Yang W, Qi F, Xie D, Shen L, Peng S, Shua C (2020) Mg bone implant: features, developments and perspectives. Mater Des. https://doi.org/10.1016/J.MATDES.2019.108259

Yusop AHM, Daud NM, Nur H, Kadir MRA, Hermawan H (2015) Controlling the degradation kinetics of porous iron by poly(lactic-co-glycolic acid) infiltration for use as temporary medical implants. Sci Rep. https://doi.org/10.1038/srep11194

Zadpoor AA, Malda J (2017) Additive manufacturing of biomaterials, tissues, and organs. Ann Biomed Eng 45:1–11. https://doi.org/10.1007/s10439-016-1719-y

Zberg B, Uggowitzer PJ, Löffler JF (2009) MgZnCa glasses without clinically observable hydrogen evolution for biodegradable implants. Nat Mater 811(8):887–891. https://doi.org/10.1038/nmat2542

Zhang Q, Cao P (2015) Degradable porous Fe-35wt.%Mn produced via powder sintering from NH4HCO3 porogen. Mater Chem Phys 163:394–401. https://doi.org/10.1016/j.matchemphys.2015.07.056

Zhang E, Chen H, Shen F (2010) Biocorrosion properties and blood and cell compatibility of pure iron as a biodegradable biomaterial. J Mater Sci Mater Med 21:2151–2163. https://doi.org/10.1007/s10856-010-4070-0

Zhao YC, Tang Y, Zhao MC, Liu C, Liu L, Gao CD, Shuai C, Atrens A (2020) Study on Fe-xGO composites prepared by selective laser melting: microstructure, hardness, biodegradation and cytocompatibility. JOM 72:1163–1174. https://doi.org/10.1007/s11837-019-03814-z

Zheng YF, Gu XN, Witte F (2014) Biodegradable metals. Mater Sci Eng R Rep 77:1–34

Zheng Y, Xu X, Xu Z, Wang J, Cai H (2017) Development of Fe-based degradable metallic biomaterials. In: Metallic biomaterials. Wiley, Oxford, pp 113–160. https://doi.org/10.1002/9783527342440.ch4

Zhu S, Huang N, Shu H, Wu Y, Xu L (2009a) Corrosion resistance and blood compatibility of lanthanum ion implanted pure iron by MEVVA. Appl Surf Sci 256:99–104. https://doi.org/10.1016/j.apsusc.2009.07.082

Zhu S, Huang N, Xu L, Zhang Y, Liu H, Sun H, Leng Y (2009b) Biocompatibility of pure iron: In vitro assessment of degradation kinetics and cytotoxicity on endothelial cells. Mater Sci Eng C 29:1589–1592. https://doi.org/10.1016/J.MSEC.2008.12.019